



First published online as a Review
in Advance on January 30, 2007

Microsampling and Isotopic Analysis of Igneous Rocks: Implications for the Study of Magmatic Systems

J.P. Davidson,¹ D.J. Morgan,^{1,2,5}
B.L.A. Charlier,^{1,3} R. Harlou,^{1,6} and J.M. Hora⁴

¹Department of Earth Sciences, University of Durham, Durham DH13LE, United Kingdom; email: j.p.Davidson@durham.ac.uk

²LGCA, UMR5205, Université Joseph Fourier, 38400 Saint Martin D'Hères, France

³Department of Earth Sciences, The Open University, Walton Hall, Milton Keynes, MK7 6AA, United Kingdom

⁴Department of Geology and Geophysics, University of Wisconsin, Madison, Wisconsin 53706

⁵Institute of Geophysics and Tectonics, School of Earth and Environment, Earth Science Building, University of Leeds, Leeds LS2 9JT, United Kingdom

⁶Danish Lithosphere Centre, Øster Volgade 10, 1350 Copenhagen, Denmark

Annu. Rev. Earth Planet. Sci. 2007. 35:273–311

The *Annual Review of Earth and Planetary Sciences* is online at earth.annualreviews.org

This article's doi:
10.1146/annurev.earth.35.031306.140211

Copyright © 2007 by Annual Reviews.
All rights reserved

0084-6597/07/0530-0273\$20.00

Key Words

crystal isotope stratigraphy, melt inclusions, recharge, contamination, Sr isotopes

Abstract

Isotopic fingerprinting has long been used to trace magmatic processes and the components that contribute to magmas. Recent technological improvements have provided an opportunity to analyze isotopic compositions on the scale of individual crystals, and consequently to integrate isotopic and geochemical tracing with textural and petrographic observations. It has now become clear that mineral phases are commonly not in isotopic equilibrium with their host glass/groundmass. Isotopic ratios recorded from core to rim of a mineral grain reflect the progressive changes in the magma composition from which the mineral crystallized. The sense of these changes and the relationship between isotopic composition and petrographic features, such as dissolution surfaces, can be used to constrain magma evolution pathways involving open system processes such as magma mixing, contamination and recharge.

INTRODUCTION: ISOTOPE RATIOS AS TRACERS

Radiogenic isotope ratios¹ are commonly used in geochemistry as petrogenetic tracers, yielding information on time-integrated elemental fractionation through processes of melting, crystallization, metamorphism, metasomatism, and contamination. Because of the time-dependent ingrowth of daughter isotopes, the isotope ratios of elements such as Sr, Nd, Hf, and Pb can be considered monitors of parent-daughter element partitioning due to past events (Dickin 2005, Faure 1986). On this basis, the spectrum of isotopic ratios can be subdivided into ranges that characterize different sources potentially involved in producing magmas. At one extreme lies depleted mantle, which has, over geological time, attained high $^{143}\text{Nd}/^{144}\text{Nd}$ (from high $^{147}\text{Sm}/^{144}\text{Nd}$), high $^{176}\text{Hf}/^{177}\text{Hf}$ (from high $^{176}\text{Lu}/^{177}\text{Hf}$), and low $^{87}\text{Sr}/^{86}\text{Sr}$ (from low $^{87}\text{Rb}/^{86}\text{Sr}$). At the other extreme is ancient continental crust with corresponding low $^{143}\text{Nd}/^{144}\text{Nd}$, low $^{176}\text{Hf}/^{177}\text{Hf}$, and high $^{87}\text{Sr}/^{86}\text{Sr}$, reflecting long-term incompatible element enrichment. Between these two extremes lie a range of mantle isotope compositions, representing end-members with different enrichments at different times, attesting to long-term plate tectonic processes, such as melt extraction and lithospheric recycling, and an even greater range of isotope ratios within the highly heterogeneous continental lithosphere.

The commonly analyzed radiogenic isotopic ratios of Sr, Nd, Pb, and Hf are not fractionated by processes of melting and crystallization² (Dickin 2005, Faure 1986) and have thus become a commonly used tool for fingerprinting source contributions in magma suites. A large body of isotopic data has been collected over the past 30 years from magmatic rocks, in progressively increasing quantity and investigative detail as both techniques and understanding have improved. For much of this time, analyses were largely restricted to powdered whole rocks, based on considerations of required sample mass and the level of detail of the investigation. Further, because whole-rock geochemical analyses for major and trace elements were carried out routinely, an isotopic estimate for the same bulk powder was an obvious consideration.

Studies employing radiogenic isotope ratios as tracers have been based largely on the assumption that fresh, young, magmatic rocks are isotopically homogeneous at the scale of minerals (and their inclusions). Indeed, homogeneity between crystal separates and groundmass has been used in the past as a test of sample integrity with respect to alteration or weathering (Halliday et al. 1984), and therefore as a validation of in situ analytical methods (Christensen et al. 1995). Technical advances in the past decade have enabled us to analyze smaller samples, with no loss of precision (Charlier et al. 2006; Davidson et al. 1998; Müller et al. 2000, 2002; Ramos et al. 2004). As a result, studies of magmatic samples have led to the realization that primary isotopic heterogeneity at the grain scale (Cioni et al. 1995, Geist et al. 1988, Simonetti & Bell 1993, Tilling & Arth 1994) and the subgrain scale (Charlier et al. 2006; Davidson et al. 2001, 2006; Harlou et al. 2005; Ramos et al. 2005) is commonplace. This contribution

¹Throughout the paper, isotope ratios refers to radiogenic isotope ratios.

²Strictly speaking, there may be very small mass fractionations, but these are effectively normalized by fractionation corrections during analysis.

reviews the theory and methods of isotopic microanalysis in igneous samples and the interpretations permitted by the data.

MINERAL-SCALE ISOTOPE DATA: WHAT DO THEY MEAN?

The basic utility of mineral-scale isotopic data as a petrogenetic tool (**Figure 1**) relies on the following assumptions:

1. When a crystal begins to grow from magma, the isotopic composition of the crystal is identical to that of the host magma from which it grows.
2. Changes in the isotopic composition of the magma will be reflected in the isotopic composition of the crystal layers that subsequently grow.

Thus, variations in isotopic composition from core to rim of a crystal are a record of the change in isotopic composition that the magma underwent during crystal growth. These principles are referred to as crystal isotope stratigraphy (CIS) (Davidson et al. 1998) and indeed follow many of the laws of simple stratigraphy, albeit at a much smaller scale. Progressive layers or growth zones from core to rim in a crystal represent a time sequence from older to younger in the evolution of the magma from which the mineral crystallized. Dissolution surfaces and significant compositional breaks represent unconformities where crystals were partly dissolved and experienced a time of no growth prior to the resumption of crystallization.

An example of how variations in magmatic composition would affect a crystal growing at a constant rate is given in **Figure 2**. In (*a*) crystal **A** growing from time t_0 to time t will have a core with an isotopic composition R_0 , and a rim with isotope ratio R , and at time t will have a bulk crystal isotope ratio of R_A . Crystal **B**, which starts growing later at time t_1 , will share the same rim isotope composition (R) but will have a different core isotope ratio (R_1) when compared with **A**. If the crystals were separated whole from the rock, they would have bulk compositions that are different (R_A and R_B , respectively), reflecting the integrated isotope ratio over the different time intervals over which they grew. The whole rock, in the most simplistic case being a mixture of **A** and **B** crystals and liquid (glass), has an isotopic ratio R_{WR} somewhere between that of the final liquid (R) and that of the lowest isotope ratio bulk crystals (R_A). The exact value of R_{WR} depends on the relative amounts of **A**, **B**, and glass, and of the concentrations of the element of which isotope ratio R is composed, in these three components. A population of crystals nucleating and growing progressively through time from t_0 to t in the magma would define a linear distribution in R versus crystal size (see inset). The larger crystals have grown for longer at the same growth rate, and will have lower whole-crystal isotope ratios, because they started growing earlier when the magma was at its lowest isotope ratio.

In **Figure 2b** evolution of the liquid is punctuated by a recharge event at t_E , which instantaneously lowers its isotope ratio. Again, crystals **A** and **B** nucleate at times t_0 and t_1 , respectively, whereas crystal **C** nucleates at t_0 but undergoes partial dissolution at t_E before resuming growth. In this case, the bulk crystal isotope ratio versus time curves mimics those of the magma with a downward spike at t_E . The crystal that began growth at t_0 would decrease its bulk isotope ratio after recharge, but the effect would be buffered compared with the dramatic change in R of the liquid because there is

CIS: crystal isotope stratigraphy

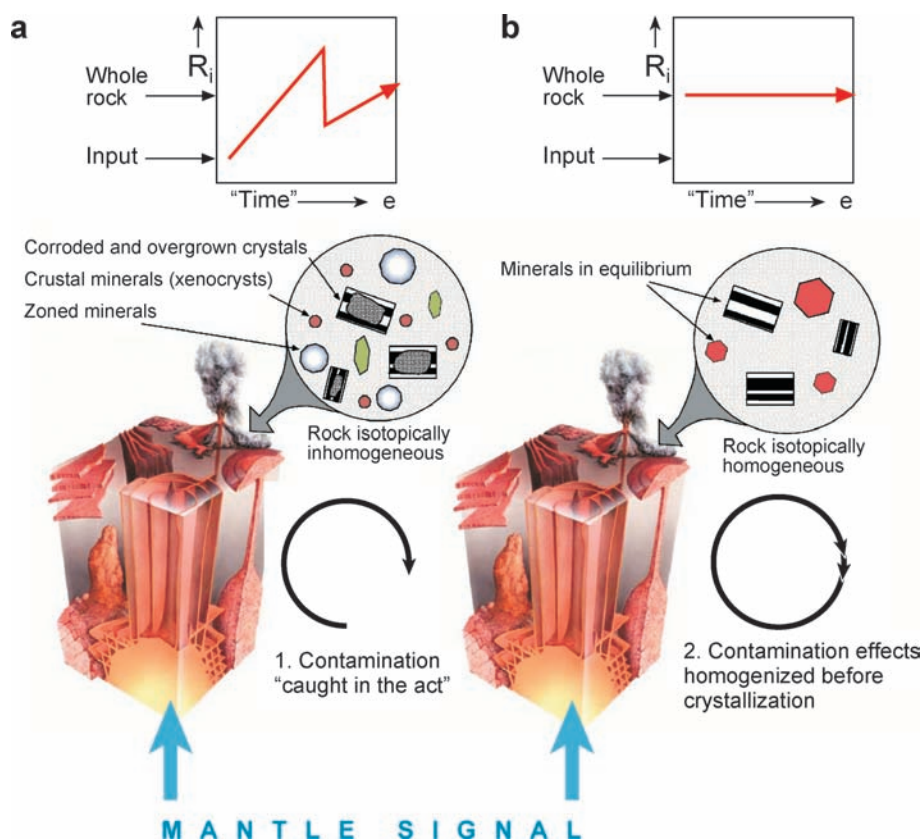


Figure 1

Schematic illustration of the principles of crystal isotope stratigraphy (CIS)—magma system schematic illustration courtesy of Gary Hincks. (a) A mantle-derived isotopic signature is transferred into a system of transport and storage in the lithosphere. Isotopic signatures are modified by processes such as contamination, magma mixing, and recharge—as represented by the arrow on the graph of initial isotopic ratio (R_i) versus time. The rock resulting at time of eruption/emplacement (e) will have a different isotopic ratio from that of the magma first introduced. But the **crystals** that grow during magma evolution (and the entrapped melt inclusions) provide a record of isotopic evolution with time. The completeness of this record depends on the time at which the crystals started (and finished) growing in the system. Early-formed crystals and crystal cores may record the earliest stages—including the original input composition, whereas late-formed crystals or crystal rims record conditions closer to those pertaining at eruption/emplacement. (b) Magmas, which may have different compositions, are homogenized before crystals begin to grow. In this case, CIS can provide no useful additional information. The key to the approach is integrating petrographic observations and data with *in situ* isotopic analysis. Note that the principles summarized here are equally valid if the isotopic variability is entirely introduced from the mantle rather than as a result of crustal processes. It should nevertheless be appreciated that the isotopic variability, however introduced, must exist at the site of crystallization. This site of crystallization is typically in the crust, as can be verified by mineral stability and mineral and melt inclusion barometry.

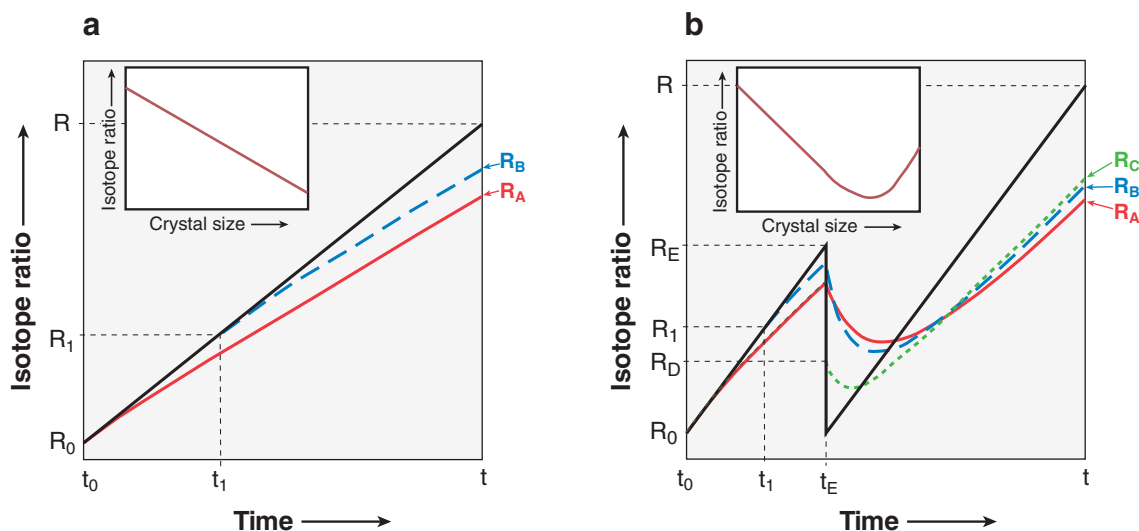


Figure 2

Schematic illustration of evolution of isotope ratio (R) of magma and integrated (bulk) single crystals grown from the magma in an open system case where the magma changes isotope composition with time. For simplicity, the rate of change of isotopic composition in the magma is illustrated as linear (perhaps reflecting progressive contamination or progressive mixing of isotopically distinct liquids). The crystal growth rate is also held constant. Insets show variation in isotope ratio with crystal size. See text for details.

already a large volume of crystal with bulk isotope ratio R_E . In contrast, crystal **B**, which began to grow at t_1 , is much smaller and therefore the bulk crystal is more sensitive to the change in isotope composition of the host liquid. It is possible also for a crystal such as **A** to undergo dissolution in response to the event at t_E . In this case, the bulk crystal R versus time curve would show a discontinuity at t_E with R dropping to a value representing the residual bulk crystal after the outer zones had been resorbed (R_D). Note how the bulk crystal isotope ratios of the late-nucleating crystal (R_B) and the crystal that undergoes dissolution (R_C) rise more steeply after t_E because the volume of crystals **B** and **C** at t_E is smaller than that of crystal **A**, so the subsequent overgrowths from the magma have a relatively greater effect. A population of crystals nucleating and growing progressively through time in this magma (undergoing a recharge/ mixing event at time t_E) would define an R versus size curve with a minimum corresponding to the size of crystals that had nucleated around t_E (see **Figure 2b** inset).

From the above schematic illustration, we can consider three separate scales smaller than that of the whole rock: bulk mineral separates, single whole grains, and the subgrain (growth zone and/or inclusion) scale. In many cases, a full appreciation of the isotopic heterogeneity in a sample requires a combination of data enveloping these scales (**Figure 3**).

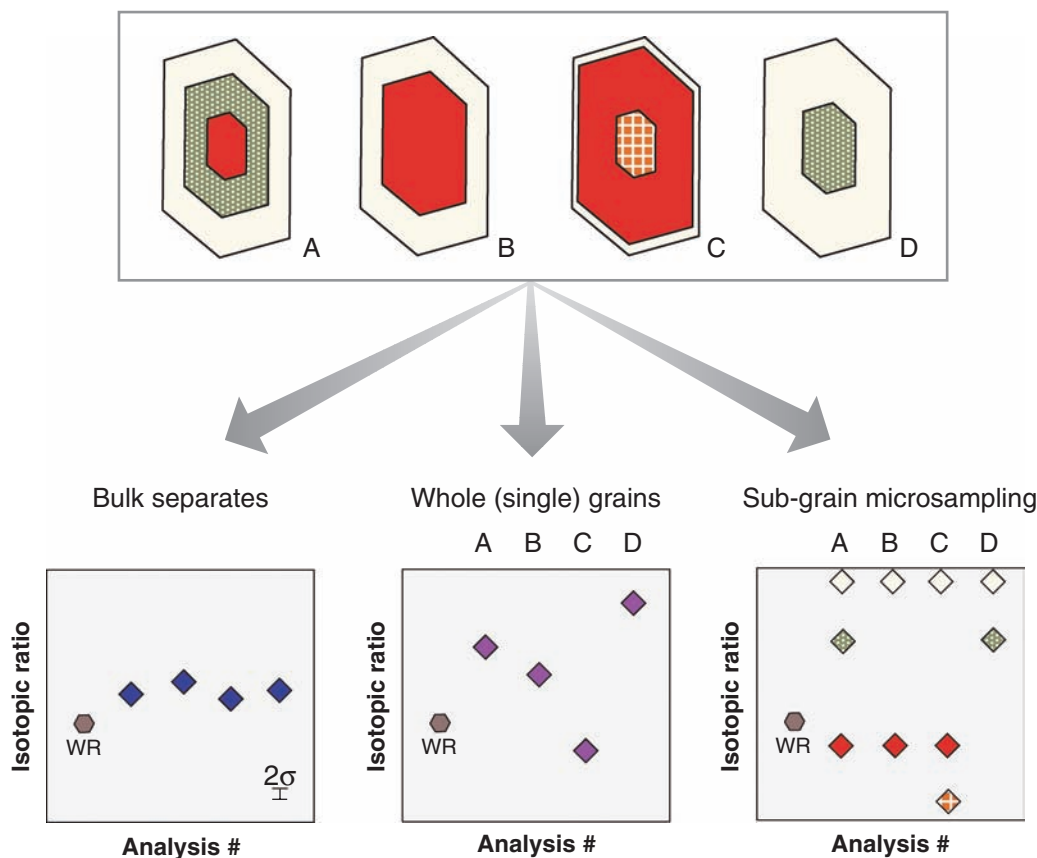


Figure 3

Schematic comparison of information provided from analysis of bulk mineral separates (*left panel*), individual whole grains (*middle panel*), and intragrain isotopic profiling (*right panel*), respectively. Illustration shows four crystals (A–D) from the same rock, each with different isotopic zoning patterns. Bulk separates average isotopic compositions and lead to limited variation compared with whole rock. Single-crystal analyses integrate the isotopic composition over the entire crystal (compare with **Figure 2**). Only with subgrain (CIS) analysis does it become clear that the color-coded zones represent discrete events, which are shared to different extents by the four crystals.

DETERMINING IN SITU ISOTOPE RATIOS: METHODOLOGY

The application of in situ isotopic profiling of natural materials extends well beyond the magma systems that are the focus of this contribution. $^{87}\text{Sr}/^{86}\text{Sr}$ profiling of shells and fish earbones (otoliths), for instance, can provide information on the growth of organisms under changing environmental conditions (Kennedy et al. 2002). Metamorphic processes (fluid flow and mineral reactions) can also be tracked through isotopic profiling of metamorphic mineral grains (e.g., Christensen et al. 1989).

As seen in **Figures 1–3**, interrogating the crystal isotopic record to recover a faithful history of magma system evolution relies on the coincidence of several criteria. The crystal species should ideally cover a crystallization range spanning as much as possible of the temperature gap between liquidus and solidus to record as much of the magmatic history as possible. Given the complex behavior of many magma systems, it helps if the crystals are not easily dissolved in response to sudden changes in composition in magmatic composition or water content, as might be expected during episodes of recharge or magma mixing (Walker et al. 1979, Grove et al. 1982). On the other hand, some response to processes (sudden changes in composition of solid solution minerals and/or partial dissolution surfaces, e.g., Ginibre et al. 2002, 2004) serve as useful petrographic guides (Wallace & Bergantz 2005). Matters are helped if crystals are sufficiently large and abundant that they can be texturally characterized or subdivided into populations. Entrapment of primary melt inclusions in the crystals is an advantage. Finally, of course, the crystals need to contain the elements of interest for isotopic analysis in sufficient abundance to make analysis feasible.

In this regard, zircons have been long-used as isotopic tracers, as they are very resilient in magma systems, contain high abundances of many isotopically relevant elements (U, Th, Pb, Hf, Sm, Nd), and can be characterized by methods such as back-scattered electron (BSE) imaging, cathodoluminescence (Pagel et al. 2000), or textural studies (Bindeman 2003) and thereby can be distinguished as distinct populations. Indeed, owing to their importance in U-Pb dating studies, zircons are effectively the subject of a distinct subbranch of studies in igneous petrogenesis and therefore are not covered in this review. The interested reader is referred to Hanchar & Hoskin (2003).

There are a number of analytical approaches in use to determine isotope ratios of Sr, Pb, Nd, and Hf in situ from minerals and glasses. The principal approaches are ion probe [secondary ionization mass spectrometry (SIMS)], laser ablation inductively coupled plasma (ICP) multi-collector mass spectrometry (LA-MC-ICPMS), and micromilling followed by wet chemistry and thermal ionization mass spectrometry (micromilling-TIMS). For the most part, these are complementary, so there is not a given method of choice. Nevertheless, it is important to choose a method commensurate with the specific problem of interest. Issues that need to be considered are

1. Analytical precision needs to be sufficient to resolve among individual sample sites within the overall range of the isotopic data. The larger the isotopic range of the system, the less stringent the need for precision. Thus, a precision of 200 ppm (e.g., 0.704 ± 0.00014) may be entirely adequate for a system with a total range in $^{87}\text{Sr}/^{86}\text{Sr}$ of 0.01 (say 0.704 to 0.714), but of no use where the total range is 0.0001 (say 0.7040 to 0.7041).
2. Spatial resolution needs to be adequate for sampling at the scale of the mineral growth zones or melt inclusions (typically 10–100 μm).
3. Interferences (the presence of isotopes of different elements with similar mass—such as ^{87}Rb on ^{87}Sr) and isotopic mass-fractionation effects (changes in isotope ratio that occur during analysis, due to, for instance, kinetic effects of

BSE: back-scattered electron (imaging)

SIMS: Secondary ionization mass spectrometry

Inductively coupled plasma (ICP): sample introduced as aerosol into an argon plasma maintained through a high temperature RF (radio-frequency) coil, which effectively ionizes the sample

LA-MC- ICPMS: laser ablation multi-collector inductively coupled mass spectrometry

LA- ICPMS: laser ablation inductively coupled mass spectrometry

MC- ICPMS: multicollector inductively coupled mass spectrometry

Micromill: mechanical drill with computer-controlled stage for extracting small amounts of rock/mineral sample (www.new-wave.com/1nwrproducts/MicroMill.htm)

TIMS: Thermal ionization mass spectrometry

evaporation from a filament) need to be characterized and corrected for accurately (e.g. Thirlwall 1997).

4. The method needs to be sufficiently efficient (time, resources) to allow enough analyses to be collected to adequately characterize the system.

Given these constraints, it is immediately clear that for a given approach there is a trade-off between spatial resolution, element concentration, and precision. Precision is strongly related to the flux of ions of a specific isotope arriving at the mass spectrometer detector. Thus, for a given precision, the higher the concentration of the element in the sample, the less of it is needed (see **Supplemental Figure 1**, follow the Supplemental Material link from the Annual Reviews home page at <http://www.annualreviews.org>)—modern TIMS instrumentation can achieve excellent precision and reproducibility for Sr samples $\ll 10$ ng (Charlier et al. 2006). Minerals with high concentrations of the element of interest can be analyzed at smaller spatial resolution than those with low abundances. Thus, Pb isotope ratios in alkali feldspars can be analyzed at small spot sizes but Pb isotope ratios in plagioclase feldspars are difficult, although not impossible, to measure (Mathez & Waight 2003), requiring much greater sample volumes to account for the lower Pb concentrations in the latter.

The second factor influencing precision and accuracy for a given ion flux at the detector is the capacity to correct confidently for interferences. SIMS and LA-ICPMS approaches are more vulnerable in this regard than micromilling followed by TIMS because the latter involves a chemical separation and purification procedure. Indeed, SIMS analysis for Sr isotope ratios is currently unable to return sufficient precision for most isotopic tracing studies because isobaric interferences of ^{87}Rb on ^{87}Sr cannot be adequately accounted for.

Many workers have opted to focus on feldspars for CIS studies. Plagioclase is a common mineral in many mafic to intermediate magma systems, crystallizing over a wide P-T range. As a solid-solution mineral with a composition sensitive to magma $P_{\text{H}_2\text{O}}$, plagioclase responds to changes in melt composition and $P_{\text{H}_2\text{O}}$ (Sisson & Grove 1993), exhibiting abrupt changes in anorthite (An) content and trace element content (Barbey et al. 2005, Costa et al. 2003, Zellmer et al. 1999) commonly accompanied by distinct and easily-observed dissolution surfaces (Ginibre et al. 2002, 2004). Most importantly, plagioclase contains high abundances of Sr, making microsampling for Sr isotope studies viable. LA-ICP-MS determinations of $^{87}\text{Sr}/^{86}\text{Sr}$ in plagioclase can now be carried out with reasonable levels of precision and accuracy (Ramos et al. 2004). Nevertheless, interferences, backgrounds, fractionation effects, and the limited flux of ions per unit time for a material of given Sr concentration mean that micromilling, chemical separation, and TIMS analysis currently provide superior accuracy, precision, and spatial resolution (Charlier et al. 2006). The limitations on the latter method are the need to maintain low blanks (typically <10 pg Sr, representing $<1\%$ of a 1 ng sample) and the unavoidably time-consuming nature of the analysis. The choice between the methods should normally be dependent on the capacity to achieve adequate precision to distinguish variations in $^{87}\text{Sr}/^{86}\text{Sr}$ within the range presented by a given magma system.

Alkali feldspar has received attention for similar reasons as plagioclase (e.g., Gagnevin et al. 2005a,b; Zellmer & Clavero 2006). It is a common mineral in evolved magmas such as granites, and, like plagioclase, typically contains abundant Sr. However, the high Rb contents of alkali feldspar can be an analytical challenge to in situ approaches, which need to account for mass interferences of ^{87}Rb on ^{87}Sr . For non-zero-age rocks (which includes all plutons), the Rb/Sr ratio must be measured simultaneously to account for radiogenic ingrowth. Thus, for alkali feldspar, spiked wet-chemical methods are currently technically easier than laser-ablation measurements for the acquisition of precise and accurate Rb-Sr data.

Alkali feldspar has the added advantage of typically containing much higher Pb concentrations than plagioclase—making Pb isotope studies also tractable through laser ablation ICP-MS or microsampling and TIMS (Gagnevin et al. 2005a). Pb isotope ratios in K-feldspar (50–100 ppm Pb) can be analyzed with ~ 100 micron laser spot sizes (Gagnevin et al. 2005a). The Pb isotopic compositions of K-feldspars as determined by LA-MC-ICPMS have consequently been used successfully in terrane correlations (Connelly & Thrane 2005) and in provenance studies (Tyrell et al. 2006).

Melt inclusions have been the subject of Pb isotopic investigations by SIMS (e.g., Saal et al. 1998, 2005; Shimizu et al. 2005) and LA-ICP-MS (Jochum et al. 2004), although sensitivity to common Pb is insufficient and only inter-isotope ratios of ^{206}Pb , ^{207}Pb , and ^{208}Pb are reported. LA-ICP-MS has also been used by Jackson & Hart (2006) to determine $^{87}\text{Sr}/^{86}\text{Sr}$ ratios on melt inclusions, although their technique is strongly limited to larger, high-Sr inclusions, typical of enriched OIB and the required interference corrections (for species of different elements or molecules but with the same mass, see Thirlwall, 1997) are extremely convoluted. Sr isotope ratio measurements on individual melt inclusions with Sr concentrations more typical of tholeiitic basalts have recently been made by Harlou et al. (2005) using micromilling-TIMS. This offline approach employs dissolution and ion exchange column chemistry enabling Rb to be separated, thus interferences are obviated and precise Sr isotope ratios can be acquired at sub-nanogram levels. A $\sim 10\%$ aliquot of the micromilled sample can also be analyzed via ICP-MS for trace element concentrations.

Much has been written in the technical literature about the various methodologies and advantages of each method (compare with summary of approaches in the mid-1990s; Neal et al. 1995), but the short summary of the relative advantages and disadvantages given in **Table 1** might be helpful to allow researchers to pick the appropriate tools to tackle specific problems. This review focuses on the relatively new approach of micromilling-TIMS. Notwithstanding the disadvantages listed in **Table 1**, it delivers high spatial resolution and the highest possible precision for a given sample size.

Interpreting Results 1: Accounting for Postcrystallization Modification of Isotopic Ratios

A simple generic template for the interpretation of isotopic profiles across crystals under ideal circumstances is given in **Figure 4**. Interpretations of isotopic data as

Table 1 Comparison of isotopic microsampling methods

Method	Spot size ¹	Advantages	Disadvantages	References
SIMS	30–50 μm	Very good spatial resolution	Fractionation and interference effects require rigorous standardization Small beam sizes produce low number of ions per unit time and limit precision	Ireland 1995
LA-ICPMS (multicollector)	Typically 50–200 μm	Rapid large numbers of samples can be analyzed in short times	Fractionation and interference effects are still not well characterized and may need more rigorous matrix-matched standard comparisons Real-time ion production limits spatial resolution (to achieve adequate precision, spot size and laser energy need to be increased as concentration decreases)	Waight et al. 2002, Ramos et al. 2004, Davidson et al. 2001
Micromill-TIMS	> 30 μm	Chemical separation and TIMS leads to excellent precision and obviates interference corrections	Offline mechanical milling and chemistry is very time consuming Blanks have to be carefully controlled and monitored, maintained at <1% Impractical to characterize very large numbers of samples.	Charlier et al. 2006

¹Area of beam/mill hole. LA-ICPMS methods may raster over a larger area to improve precision. Depth of SIMS analyses is a few micrometers, whereas LA-ICPMS spot is deeper (but depth is typically less than hole width to prevent significant signal decay and more severe fractionation effects). Micromill-TIMS hole depths are also less than width—in the most recent approaches described by Charlier et al. (2006) drills are tapered and therefore volume is dominated by the shallow part of the hole.

reflections of magmatic evolution do, however, rely on accounting for modification processes, such as radiogenic daughter ingrowth and diffusional reequilibration.

Ingrowth of daughter isotopes over time is a problem associated with high parent/daughter ratios and/or significant time between crystallization and analysis of the crystal. This can be accounted for by applying an age correction. The efficacy of the age correction depends on accurate and precise determination of the parent/daughter isotopic ratio and of the sample age (see **Supplemental Figure 2**).

Diffusion operating within crystals at magmatic temperatures will cause the isotopic compositions of mineral phases that make up a rock to equilibrate to some degree. At feasible magmatic conditions, relatively rapid crystal growth rates typically mean that only the outer few micrometers of a crystal are in diffusive communication with the melt over short timescales of the order of years (Brady 1995). For a crystal to completely equilibrate with a changing magma isotope composition as it grew, it would need to be held at high temperatures for thousands to tens or even hundreds of thousands of years. We can infer that this has not happened because trace element profiles across phenocrysts often show considerable deviation from equilibrium

Phenocryst: mineral that has crystallized directly from the magma (rock) in which it is hosted

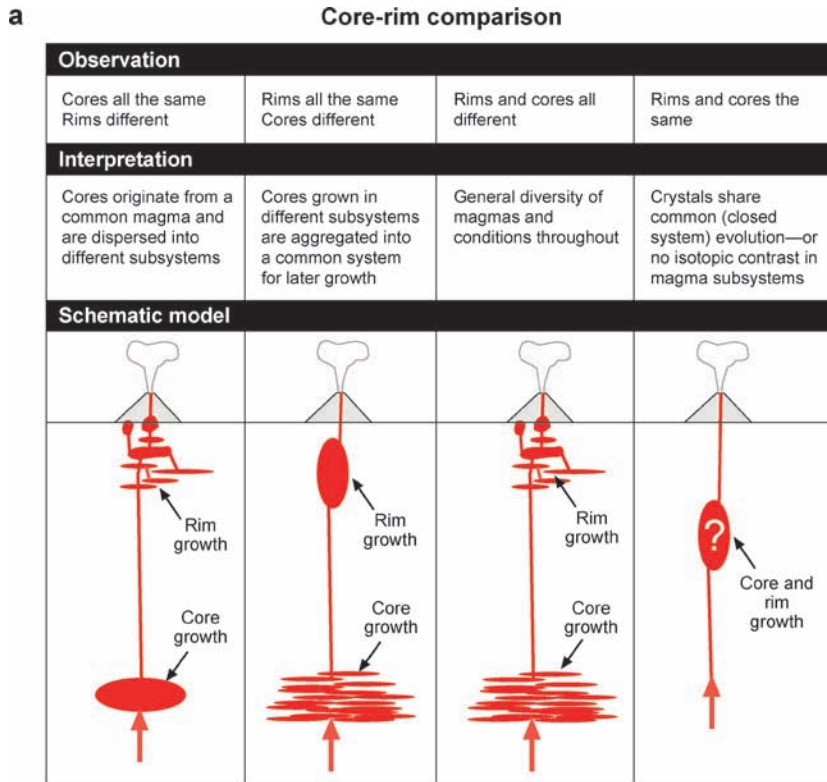
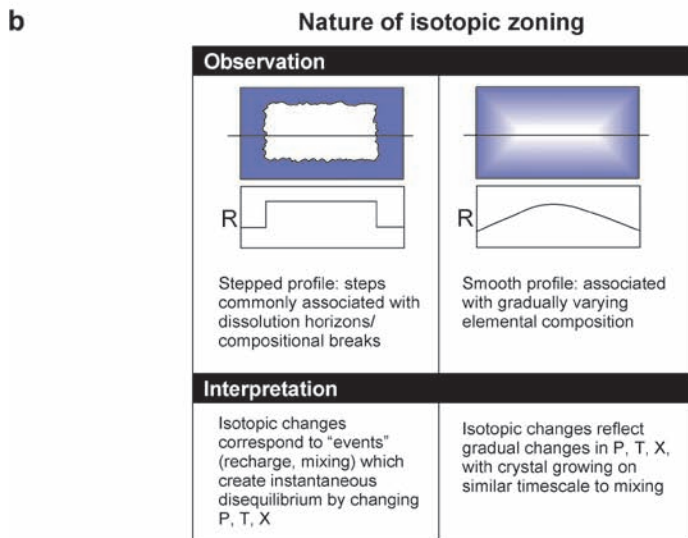


Figure 4

General representation of possible interpretations of CIS data based on (a) comparison of isotope ratios among cores and rims of crystals and (b) nature of the isotope profile zoning. In (a), the schematic models have no explicit association with particular depths in the crust [other than magmas tend to ascend so in cases of polybaric crystallization cores will crystallize earlier (deeper) and rims later (shallower)]. In (b), R represents schematic isotope ratio profile across the section line in the crystal where color shading represents isotope ratio.



DIFFUSION AND TIMESCALES

Diffusion distances inside the crystal are proportional to \sqrt{Dt} , whereas growth distances are proportional to Gt (D = diffusivity, G = growth rate, and t = time). At short timescales, diffusion is dominant, but as t grows, Gt overtakes \sqrt{Dt} in importance. For example, in a mineral of intracrystal diffusivity, $D = 1 \times 10^{-20} \text{ m}^2\text{s}^{-1}$, growing at a rate of $G = 1 \times 10^{-13} \text{ ms}^{-1}$, growth effects are more significant than diffusion effects at timescales of over $1 \times 10^6 \text{ s}$, or roughly 12 days, corresponding to a layer of crystal 100 nm thick. Thus, effects of shorter duration than 12 days occurring during crystal growth will suffer from some amount of diffusional interaction with the surrounding magma during the period of growth. If growth is slower or intracrystalline diffusion faster, this critical timescale increases. If in the above case the growth rate was ten times slower, the critical timescale is 100 times greater at $1 \times 10^8 \text{ s}$ (about three years) and the band disrupted by diffusion during growth is wider, at one micrometer. These length scales are, for plagioclase at least, generally much smaller than the smallest analyzable zone size, and so the assumption that the crystal was in isotopic equilibrium with melt at the time and point of crystallization can be regarded as valid.

(Costa et al. 2003, Morgan et al. 2004, Zellmer et al. 1999), and tracer diffusion is effectively faster at attaining near-equilibrium than the required volume diffusion for isotopic resetting (see sidebar Diffusion and Timescales).

We can therefore be confident that mineral scale (at least $\geq 50 \mu\text{m}$) isotopic variations in volcanic rocks effectively record a snapshot of the magma system prior to the time of eruption. Perhaps surprisingly, the few studies that exist of mineral-scale isotopic studies in plutonic rocks, which have cooled more slowly, demonstrate that minerals in plutonic rocks are also not isotopically equilibrated (Gagnevin et al. 2005a,b; Tepley & Davidson 2003; Waight et al. 2000, 2001) (see **Supplemental Figure 3** for the relationships among temperature and composition that control diffusivity in minerals and equilibration timescale). In the case of plagioclase, the higher emplacement temperatures of more mafic intrusions are offset by lower diffusivities of Sr in the more anorthite-rich plagioclase, compared with those of albite-rich plagioclase, which characterizes lower temperature granites (Cherniak & Watson 1994, Giletti & Casserly 1994).

Interpreting Results 2: Integrating Isotope Data with Major and Trace Element Data

The true potential of isotopic microanalysis as an investigative tool is only fully realized when it is combined with trace-elemental, major-elemental, or textural data (e.g., Müller 2003) informative of other processes and factors (**Table 2**). Work based

Table 2 Petrographic and geochemical approaches that may be integrated to fully appreciate magma system evolution

Technique	Information
Microisotopic studies	<ul style="list-style-type: none"> • Isotopic evolution of magma system • Not affected by short-term fluctuations in intensive parameters such as P, T, H₂O, therefore, gives a relatively simple view of a single, changing parameter
CSD	<ul style="list-style-type: none"> • Population growth history—gives time aspect on population development • Significant changes in crystallization behavior or mixed populations can be seen in kinked CSDs
BSE imaging	<ul style="list-style-type: none"> • Compositional information [e.g., feldspar crystals (Ginibre et al. 2002)] • Textural features such as dissolution surfaces representing changes in T, P, H₂O
3-D reconstruction (e.g., X-ray CT, serial section)	<ul style="list-style-type: none"> • Direct information on size shape and distribution of crystals (e.g. Mock & Jerram 2005, Gualda 2006) • Identification of mixed populations • Provides ideal sampling strategy for micro analysis
EPMA and SIMS analysis	<ul style="list-style-type: none"> • Measurement of major, minor, and trace elemental abundances at the microscale, indicative of the chemical changes associated with textural changes. Allows processes to be associated with the variations seen in BSE imaging • Due to the small scale of the analyses, diffusion profiles are often observable that can yield timescale information (Morgan & Blake 2006)
LA-ICPMS	<ul style="list-style-type: none"> • Trace elemental variations, albeit at a larger scale than via SIMS or EPMA. An advantage is speed of analysis, but the technique is destructive and leaves less material for isotopic sampling. Diffusion profiles are not readily measurable via LA-ICPMS owing to the large size of analysis points
Cathodoluminescence	<ul style="list-style-type: none"> • Good for understanding internal crystal structure. Also, different colors may be associated with different processes or paragenesis and so may aid the subdivision of samples with reference to chemical data (e.g. Ginibre et al. 2004)

on major-element contents of feldspar crystals has attempted to address similar problems, considering crystals in terms of their relationship to a “phylogeny” (Wallace & Bergantz 2002). In this conceptual case, crystals all share the same recent history—potentially represented by the rim compositions grown immediately before eruption—but diverge in common characteristics as their histories are traced back through time from rim to core. Isotopic work can simplify this process in terms of removing the high-frequency fluctuations from the signal, and for the relatively straightforward system of Stromboli Volcano this was achieved for a single lava sample (Morgan et al. 2005)—see case study below, yielding information on crystallization versus contamination and cumulate incorporation processes. Comparing the stratigraphies of several crystals in a given sample may therefore give a better overall record of the evolution of the magma, which the rock represents, but remains highly time-consuming work. The principles and utility of isotopic microanalysis in volcanology can be summarized in a few illustrative case studies, presented below.

Cumulate: aggregation of minerals that have crystallized from, and subsequently been removed/isolated from, a magma

SINGLE-CRYSTAL VERSUS CORE-TO-RIM DATA (CASE STUDIES FROM EL CHICHÓN, NAGUARUHOE, AND TAYLOR CREEK)

To illustrate the theoretical cases discussed above, we present case studies from contrasting magma systems. At Ngauruhoe Volcano (New Zealand) and El Chichón (Mexico), isotope heterogeneity in recently erupted basaltic andesite and trachyandesite lavas, respectively, argue for open system processes occurring during differentiation (Hora 2003, Tepley et al. 2000). At Ngauruhoe, $^{87}\text{Sr}/^{86}\text{Sr}$ data from single plagioclase crystals, albeit limited, reveal crystal cores with lower $^{87}\text{Sr}/^{86}\text{Sr}$ and crystal rims with higher $^{87}\text{Sr}/^{86}\text{Sr}$ (**Figure 5a**). This observation is consistent with growth of crystals from a progressively more contaminated magma. In a simple model (**Figure 2a**) we would expect larger plagioclase crystals to have a lower (intergrated) single-grain $^{87}\text{Sr}/^{86}\text{Sr}$ than the smaller ones, and this is indeed observed for eruptions in 1870, 1949, and 1954. We would also expect the groundmass (representing the liquid) to have a higher $^{87}\text{Sr}/^{86}\text{Sr}$ than the minerals. Generally, this is the case. Where analyzed, clinopyroxene has relatively low $^{87}\text{Sr}/^{86}\text{Sr}$, suggesting that it crystallized mainly during the earlier stages of evolution when the magma had relatively low $^{87}\text{Sr}/^{86}\text{Sr}$. There are, however, difficulties in such a simple explanation. In the 1974–75 eruption, for instance, the small plagioclase crystals have the lowest $^{87}\text{Sr}/^{86}\text{Sr}$. This can be explained by sequestering of early-formed phases into cumulates with later remobilization just before eruption, or simply by mixing of crystal populations that have undergone separate differentiation events in different parts of a magma system. The observations implicate open system differentiation, but underscore the need to (a) obtain isotopic data for a large population of crystals in any given rock and (b) combine these data with textural and other geochemical observations, which will help constrain the process or processes that dictated magma evolution pathways (**Table 2**).

At El Chichón Volcano (Mexico), a similarly diverse suite of isotope data from mineral separates of the 1982 eruption (Tilling & Arth 1994) has been investigated at the single-crystal scale (**Figure 5b**). The El Chichón plagioclase population is more conducive to in situ isotopic study than that at Ngauruhoe because plagioclase crystals are considerably larger (up to 5 mm compared with typically <1 mm), and Sr concentrations are very high (1500–2000 ppm compared with 200–700 ppm). Tepley et al. (2000) report consistent core-to-rim variations for El Chichón feldspars, with rim $^{87}\text{Sr}/^{86}\text{Sr}$ ratios lower than those of the core. Thus, the magma from which plagioclase rims grew was apparently less contaminated than that from which the cores originated. Furthermore, changes in isotopic composition from core to rim appear to correlate with textural features (dissolution surfaces), which suggests that changes in isotope composition of the magma reflect discrete events such as magma recharge, that produces an environment in disequilibrium with the growing crystal (Davidson et al. 2001, Davidson & Tepley 1997, Tepley et al. 2000).

Finally, in a rhyolite dome of the Taylor Creek Complex (New Mexico, USA), core-to-rim isotopic traverses in single sanidine crystals can be compared with single-crystal data across the spectrum of sizes (**Figure 5c**; Knesel et al. 1999). In this example, the single crystal data exhibit a pattern of increasing $^{87}\text{Sr}/^{86}\text{Sr}$ with size

up to a maximum value, after which $^{87}\text{Sr}/^{86}\text{Sr}$ decreases. Single-crystal data for three individual sanidines of different size show the same overall pattern, with $^{87}\text{Sr}/^{86}\text{Sr}$ low in the core, increasing rimward to a maximum value, then decreasing toward the rim. The single-crystal data set and the core-to-rim traverses are consistent with growth of the crystals in a progressively contaminated rhyolite magma, followed by growth in a magma with decreasing $^{87}\text{Sr}/^{86}\text{Sr}$. The cause of decreasing $^{87}\text{Sr}/^{86}\text{Sr}$ was suggested by Knesel et al. (1999) to be recharge and mixing with less contaminated rhyolite (cf Hervig & Dunbar 1992). In contrast with the El Chichón case, growth appears to take place during mixing, suggesting that mixing might be more protracted owing to the high viscosities of the rhyolite liquids. At El Chichón, mixing led to dissolution and subsequent crystal growth from a hybridized liquid with a lower but relatively constant $^{87}\text{Sr}/^{86}\text{Sr}$.

In all three cases, mixing of melts of different isotopic composition appears to be an important process (**Figure 5d**). At Ngauruhoe and El Chichón, the mixing is reflected in disequilibrium textures between growth zones. At Ngauruhoe, the magma mixed is more differentiated and has higher $^{87}\text{Sr}/^{86}\text{Sr}$, whereas at El Chichón (repeated) magma mixing appears to reflect recharge by a more primitive melt. At Taylor Creek, the mixed magma was evidently similar in composition (rhyolitic) and did not produce disequilibrium features, but was isotopically distinct, being lower in $^{87}\text{Sr}/^{86}\text{Sr}$.

PHENOCRYSTS, XENOCRYSTS, AND ANTECRYSTS

The case studies summarized above demonstrate that a rich and detailed record of magma evolution can, in principle, be extracted by applying isotope studies at the mineral-grain scale. However, in all three examples, a single, simple pathway of magma evolution cannot account for all of the observed data. Models such as those in **Figure 2** predict that all crystals should have the same isotopic compositions at their rims (identical to the host groundmass, and that smaller crystals should typically have higher bulk $^{87}\text{Sr}/^{86}\text{Sr}$ than larger ones. We propose that the crystals found in many magmatic rocks may not have shared common histories and crystallized from the liquid (glass/groundmass) in which they are now hosted, but rather represent a liquid (glass/groundmass) laced with a crystal cargo that has been inherited from liquids that existed at different places and times in the magma system. The crystals are then not true phenocrysts. Neither are they strictly xenocrysts, as they are grown and recycled from closely related progenitor magmas rather than accidentally incorporated from older unrelated wallrocks. W.E. Hildreth (personal communication) has suggested the term “antecryst” to denote phases that originate in the magma system but are not true phenocrysts (cf Charlier et al. 2005). On this basis, we propose that magmatic rocks can be represented by mixtures of liquid (solidified to glass/groundmass), recycled antecrysts, and true phenocrysts (**Figure 6**). Most microlites, grown during the last stages of eruption, are of similar composition to true phenocryst material (Tepley et al. 1999). Large crystals, which have traditionally been referred to as phenocrysts, can be shown in many cases to be antecrysts, albeit commonly rimmed by equilibrium phenocryst material. In the representation of **Figure 6**, closed systems

5a Nguaruhoe North Island, New Zealand 	Magma composition Basaltic andesite
	Eruption age(s) Cone active for 2000 years, samples from 4 eruptions 1870–1975
	Reference(s) Hobden 1997, Hobden et al. 1999, 2002, Hora 2003

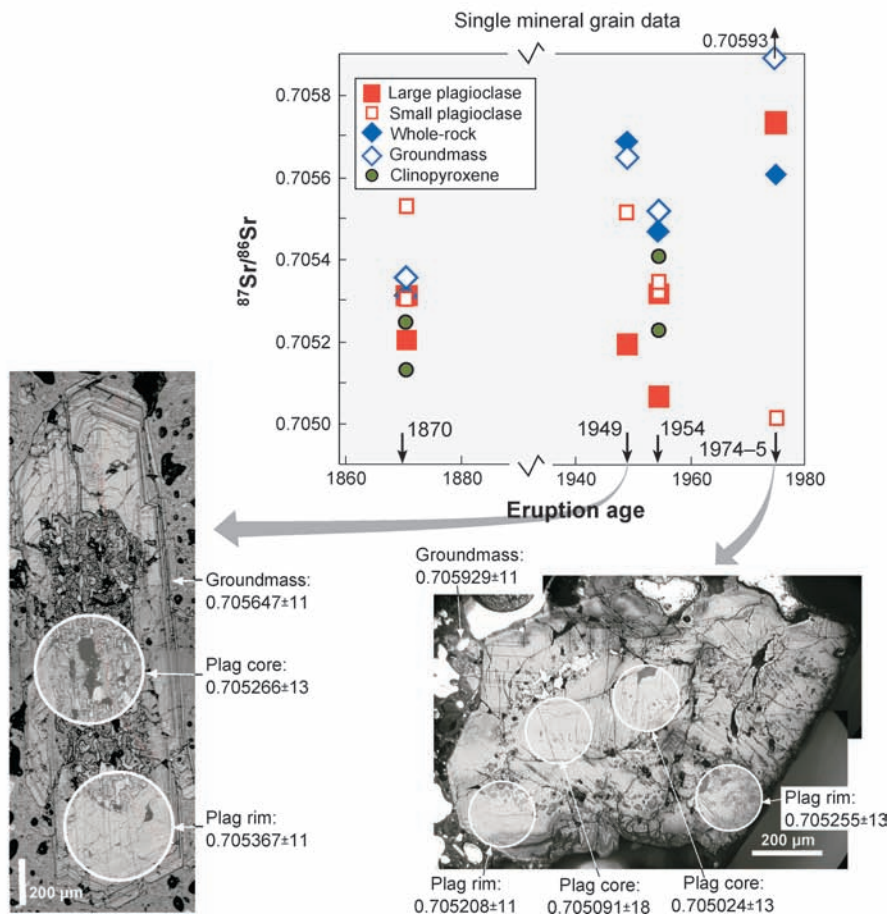


Figure 5

Case studies of whole crystal versus single crystal isotope variations. (a) Nguaruhoe (after Hora 2003), (b) El Chichón (Tepley et al. 2000), (c) Taylor Creek (Knesel et al. 1999). (d) Summarizes schematically the simple magma evolution pathways inferred for the three systems from combining CIS with textural observations and major element (electron microprobe) data.

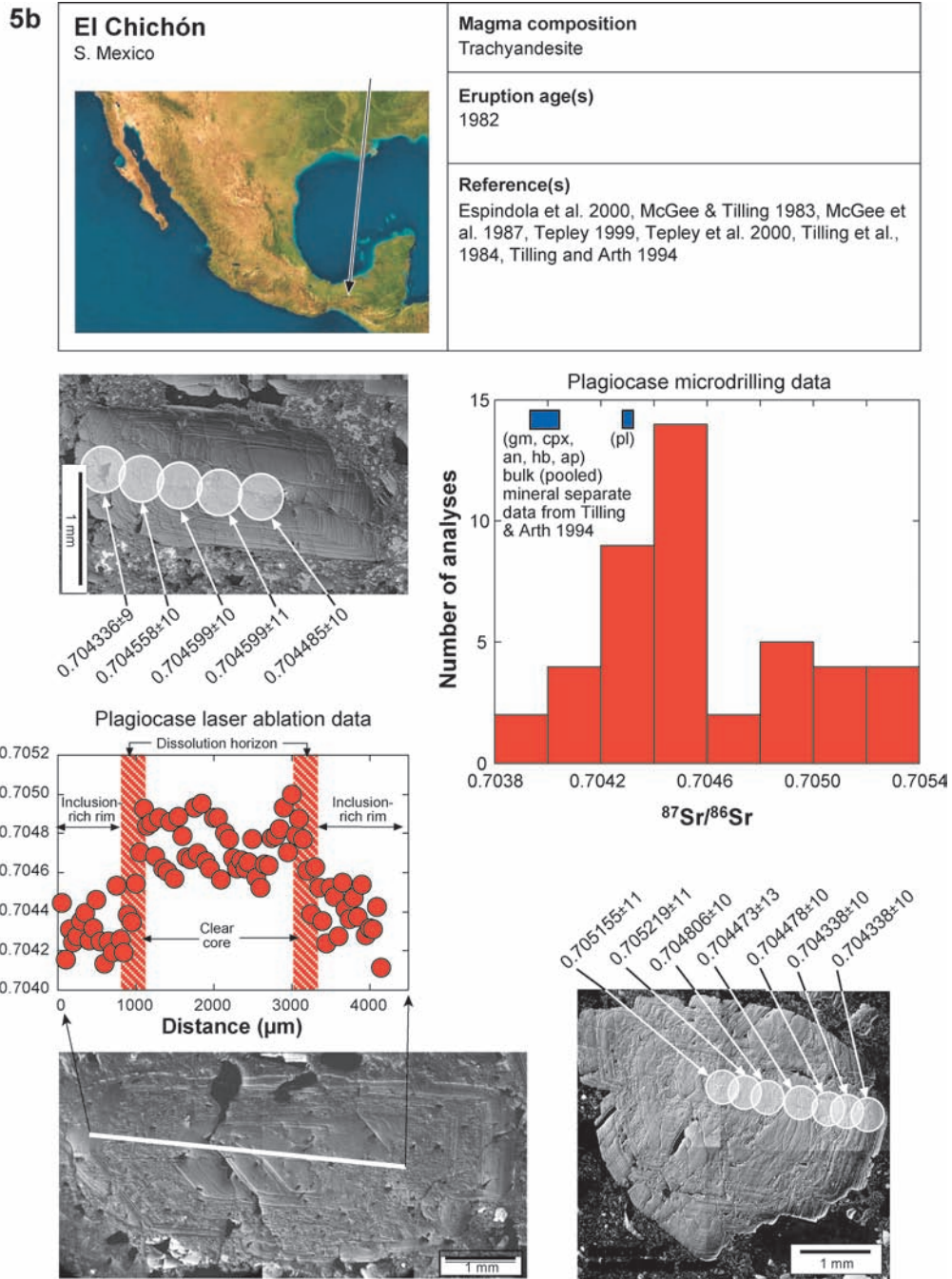


Figure 5

(Continued)

<p>5c Taylor Creek New Mexico, USA</p> 	<p>Magma composition Rhyolite</p>
	<p>Eruption age(s) 27.9 Ma</p>
	<p>Reference(s) Duffield and Ruiz, 1992, 1994; Knesel et al., 1999</p>

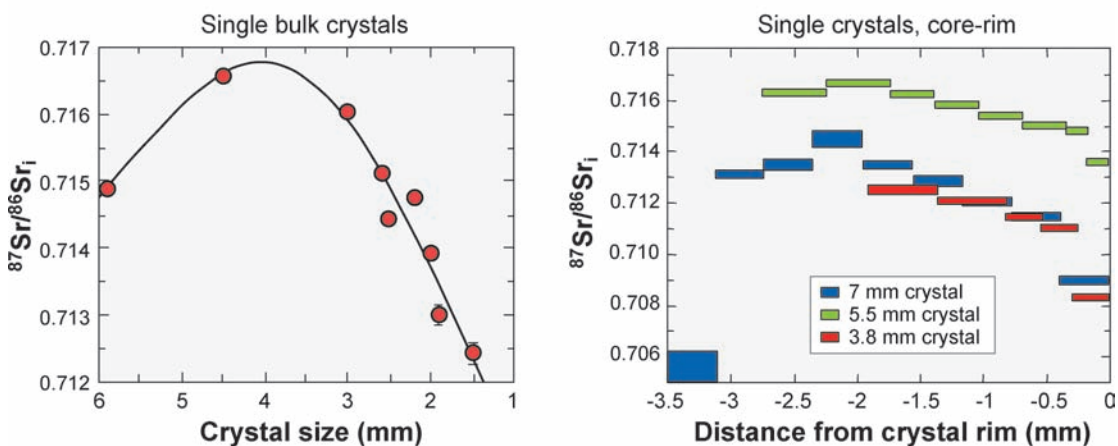
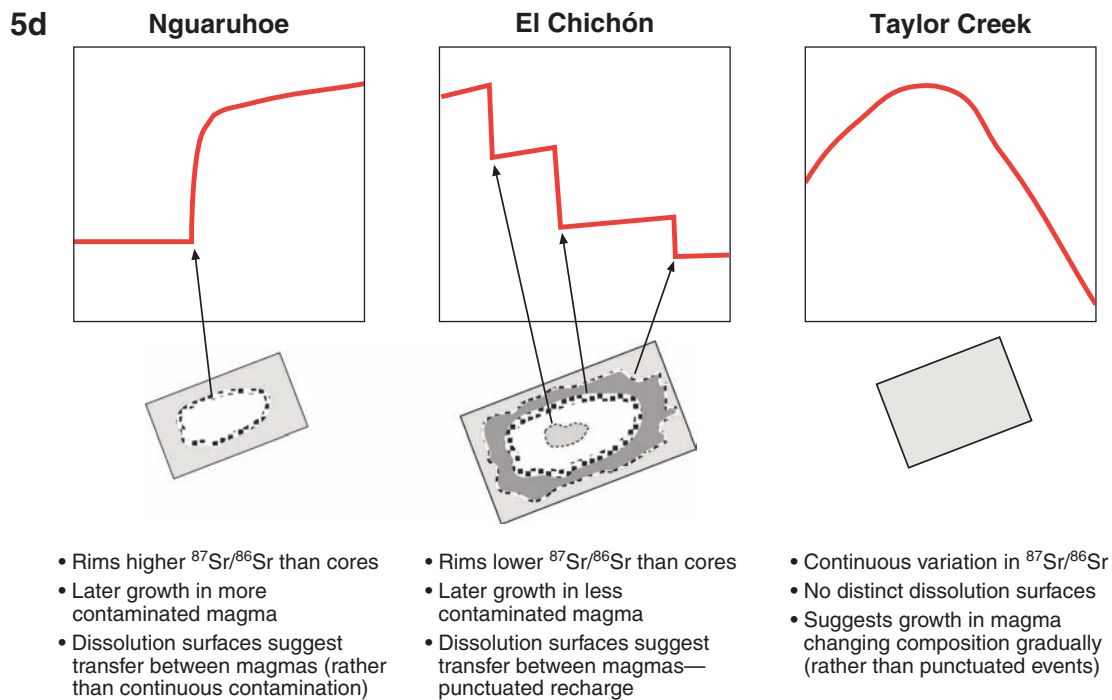


Figure 5
(Continued)

lie only along the line P-L and would be expected to be isotopically homogeneous at the mineral scale. All other magmas are amenable to investigation by CIS provided there is measurable isotopic diversity within the system. To apply CIS however, crystal types ideally need to be distinguishable on the basis of petrographic criteria. True xenocrysts—material accidentally picked up from older preexisting wallrocks—can usually be identified petrographically and are easily identified using the in situ microanalytical isotopic approaches discussed above (Chadwick et al. 2005, Perini et al. 2003, Waight et al. 2001).

This realization is not necessarily new—researchers studying andesites have for many years recognized the disequilibrium textural features and mineral compositions of phases in orogenic magmas, and have used this observation to underscore the importance of magmatic mingling and mixing (e.g. Bacon 1986, Clynne 1999,

**Figure 5***(Continued)*

Eichelberger 1978, Koyaguchi 1986). What CIS does bring to the debate, however, is the capacity to fingerprint and quantify contributions from different components in the magma system (primary magmas, crustal melt, mixed melts, xenocrysts), and to distinguish these open-system effects from those that may be due simply to changing storage conditions such as T and $P_{\text{H}_2\text{O}}$.

WHAT SIGNIFICANCE HAS THE ISOTOPIC COMPOSITIONS OF CRYSTAL RIMS?

In our simple conceptual model (**Figure 2**), the outermost rims of the crystal are in equilibrium with the isotopic composition of the host magma—represented in the magmatic rock as glass or groundmass. As we have seen from the case studies summarized above, crystal rims do not always share the isotopic composition of the groundmass. Of course this may in part be due to the resolution at which we can sample the crystal rims; if less than approximately $50\ \mu\text{m}$, the analytical method used (micromill or laser) will likely be sampling a mixture of rim material and internal zone(s). Nevertheless, the use of textural features to constrain sampling strategies means that we can be aware of this limitation, and, in general, we can be confident

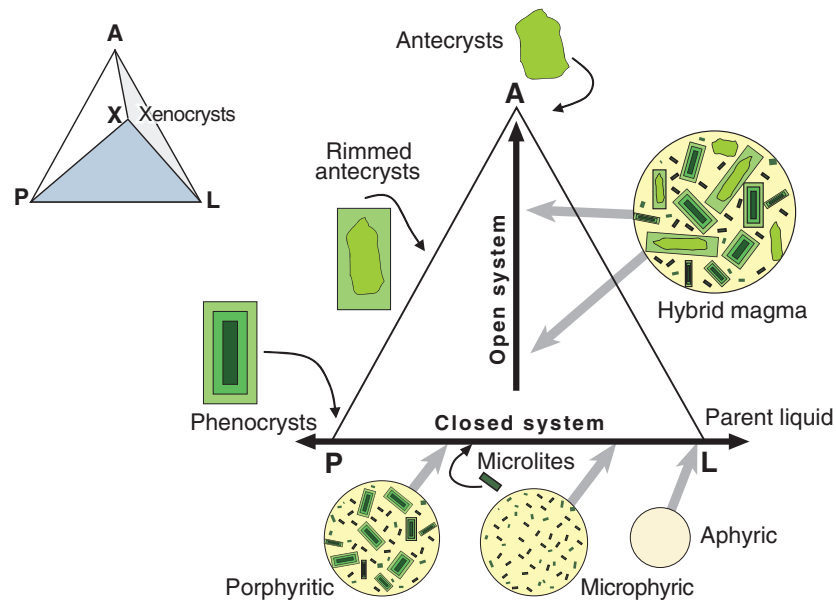


Figure 6

Classification of magma crystal populations according to their relationship to the magma. Most rocks can be represented as a mixture of liquid (L), true phenocrysts (P), and antecrysts (A), although a tetrahedral extension of this approach could be used to take into account xenocrysts (X), as illustrated top left. We define antecrysts as crystals that are related to the magma system, but not directly crystallized from the host magma in which they are finally contained.

that we are sampling a texturally consistent rim inferred to be in equilibrium with the groundmass of the host. Thus, isotopic differences between rim and host magma imply that either (a) the host magma changes its isotopic composition more quickly than crystal growth on the scale that we can sample ($\sim 50 \mu\text{m}$) can reflect such changes, or (b) crystals have been recently brought into contact with the liquid in which they are now hosted, and, at the time of eruption, are either undergoing dissolution or have had insufficient time to reequilibrate to the new conditions and resume growth.

In either case, if crystal growth rates are as reported in the literature (e.g., 10^{-11} to 10^{-14} ms^{-1} for plagioclase) then events such as contamination, cumulate recycling, and magma mixing must take place over timescales much less than 150 years (the maximum time it would take for plagioclase to grow $\sim 50 \mu\text{m}$). Although it is possible that a crystal edge, like an unconformity, is actually dissolved/eroded over longer timescales, this is unlikely because dissolution is typically a faster process than crystal growth (Tsuchiyama 1985). In fact, these magmatic processes may well be the progenitors to magmatic eruptions, which occur over weeks to years and are recorded in geophysical and geochemical precursors such as seismicity and gas fluxes. The prospect exists that magmatic events preceding eruptions and dictating the nature, style, and size of eruptions may be recorded in the crystals disgorged on eruption (Morgan et al. 2004, 2006; Morgan & Blake 2006).

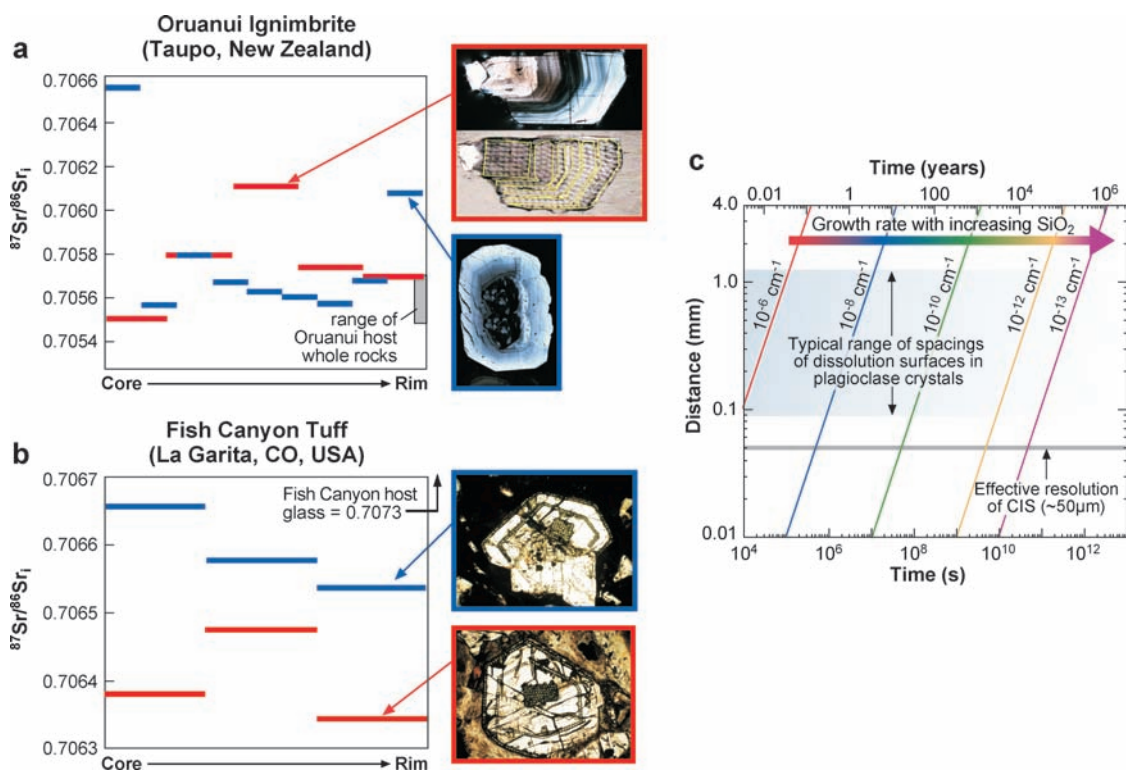


Figure 7

Core-to-rim $^{87}\text{Sr}/^{86}\text{Sr}$ profiles of two feldspar crystals from the Oruanui Ignimbrite, New Zealand (a) and two from the Fish Canyon Tuff, Colorado, USA (b). Note sampling pits in 3 of the four feldspars analyzed (the other is photographed prior to sampling). Note also in the case of the (upper) Oruanui feldspar the need for careful petrography integrated with CIS—for this crystal the core is clearly not in the “middle” of the crystal, which has been broken during explosive eruption. Panel (c) shows crystal growth rates, which typically become slower as magmas are more evolved (cooler, more SiO₂-rich and more viscous; e.g., Cashman 1990). If growth rate is known (or estimated) then features on crystals (width of rims, distance between dissolution surfaces) can be related to time.

In this regard, it is important to note that rim-host disequilibrium has been observed in many crystals from large-volume ignimbrites (**Figure 7**). Of the two microsampled crystals shown from the Oruanui Ignimbrite (New Zealand), one has a rim in isotopic equilibrium with the groundmass glass (as approximated by the crystal-poor bulk rock) and the other has a rim that is quite distinct. Both feldspars shown from the Fish Canyon Tuff (USA) have rims far from equilibrium with the host liquid (glass). The sampling scale of the crystal rims can be appreciated from examination of the distribution of the micromill pits (which are ~50 μm diameter). A simple consideration of growth rates summarized in **Figure 7c** suggests that these crystals with isotopically distinct rims were unlikely to have been in contact with the melt represented by the immediately adjacent glass for more than ~10,000 years. This observation is

Crystal size distribution

(CSD): a means of quantifying the 3-D crystal population in terms of the population density at different size intervals

at odds with models advocating protracted (>100,000 years) closed-system evolution to incubate large volumes of silicic magma (e.g., Christensen & DePaolo 1993, Christensen & Halliday 1996, Halliday et al. 1989), but does corroborate suggestions that some large-volume silicic systems [such as Fish Canyon (Bachman et al. 2002) and Taupo (Charlier et al. 2005)] represent remobilized plutons.

Figure 7c gives a useful indication of the potential applicability of CIS to unraveling the timescales of magmatic processes. Crystals in basaltic and andesitic systems can grow to sizes of the order ~1 mm in months to years. Dissolution surfaces in crystals are typically spaced at a few hundred micrometers or less, again the time taken to grow each zone between dissolution surfaces is of the order of months to years, although the time represented by the dissolution surface itself, like unconformities in the sedimentary record, may be much longer. The application of diffusional analysis techniques to elemental variations across dissolution horizons brings an opportunity to determine residence times of crystals in magmas. The diffusion profile (elemental or isotopic) can be assessed in light of an independently determined magmatic temperature and using appropriate published diffusivities. In this regard, elemental techniques provide better time resolution (e.g., Costa & Dungan 2005, Morgan et al. 2004, Morgan & Blake 2006, Zellmer et al. 1999) than equivalent modeling for isotopic ratios (Davidson et al. 2001, Morgan et al. 2005, Ramos et al. 2005) because the analytical resolution for trace elemental analysis is spatially finer ($\ll 50 \mu\text{m}$), shows a greater contrast (tens of percent for trace elements versus fractions of a per mil for isotope ratios), and the diffusing species studied are not limited to those of isotopic significance, meaning that a range of timescales can be investigated owing to differing diffusivities of elements with a range of partitioning behaviors.

INTEGRATING CIS WITH ROCK AND MINERAL TEXTURES (CASE STUDY FROM STROMBOLI)

It is implicit that petrographic observations are fundamental to providing a context for interpretation of in situ isotopic determinations to constrain magma evolution (**Table 2**). The evolution of the mineral assemblage and its petrographic textures goes hand in hand with the isotope stratigraphy. Quantitative approaches to measuring mineral distributions and textures developed in recent years have been instrumental in constraining the evolution of magmas. Crystal size distributions (CSDs) (Higgins 2000, Marsh 1988) can be used to determine growth rates (from the slopes) and to identify mixing of crystal populations (from segments with different slopes, e.g. Jerram et al. 2003). It seems opportune, therefore, to combine the information provided by CIS with that gleaned from textural analysis.

To illustrate the integration of different techniques with isotopic microanalysis, we present some results from Stromboli Volcano, Italy (**Figure 8**). Thick sections were prepared and crystals analyzed with electron microprobe and BSE imaging. Textures were quantified by CSD measurements prior to micromilling-TIMS of selected crystals. Three crystals were selected for analysis, one of which is shown in **Figure 8c,d**. The BSE image as shown was calibrated against the microprobe data (Ginibre et al. 2002) and a high-resolution anorthite profile was extracted from the

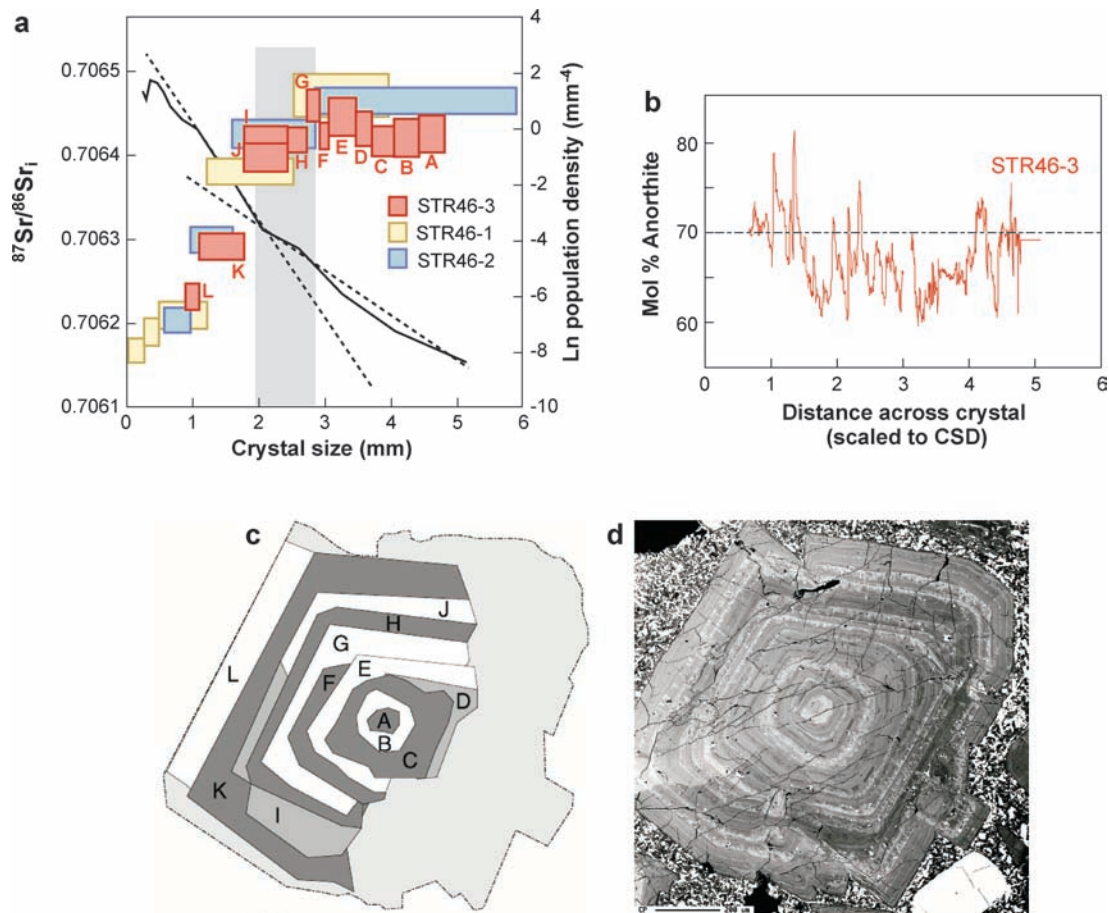


Figure 8

Integration of CIS profiles with crystal size distribution (Morgan et al. 2005). (a) The CSD is for a 26 kyr lava from Stromboli Volcano and shows two segments of different slope (*emphasized by dashed lines*). The overlain CIS profiles for three different crystals (*distinguished as different color shading*) show a change from constant $^{87}\text{Sr}/^{86}\text{Sr}$ at ~ 0.70645 in the cores to gradually decreasing $^{87}\text{Sr}/^{86}\text{Sr}$ towards the rim. Vertical thickness of CIS boxes represent precision on the isotopic ratio. Horizontal width represents sampling thickness (corrected for three-dimensional effects and shifted to correspond with the other crystals). The most detailed traverse is shown for crystal STR46-3 as zones A–L. (b) An electron microprobe profile of An content, (c) a sketch of definable growth zones as sampled by micromilling, and (d) a backscattered image of that crystal (STR46-3) are also shown.

image (**Figure 8b**). $^{87}\text{Sr}/^{86}\text{Sr}$ profiles for all three crystals are shown after processing to integrate them with the CSD, giving an isotopic-CSD plot, or ICSD (**Figure 8a**).

Note that the three crystals do not share the same isotopic compositions at their rims. Portions of the crystal population are interpreted to represent a crystal cargo that has been mechanically incorporated into the liquid in which they are now frozen,

and with which they only share a portion of their mutual evolutionary history. One crystal has a rim composition in equilibrium with the host groundmass, the others have higher $^{87}\text{Sr}/^{86}\text{Sr}$ rims, suggesting that they have been isolated from the magma earlier (and therefore did not experience the most recent growth episode). This observation allows us to shift the isotope profiles (and stretch them) so that they overlie each other and represent a common time line from right (core) to left (rim). The timeline of **Figure 8a** shows a marked increase in isotopic ratio of the crystal core between crystal lengths of 1 mm and 2.5 mm. The onset of the change in ratio (vertical gray band) correlates with the presence of a pronounced kink in the CSD (emphasized by the dashed line segments in **Figure 8a**) between 2 mm and 2.5 mm crystal size. Plateau ratios could therefore be due to (a) an inherited population of crystal cores and (b) a population of crystals of size less than 2.5 mm, along with rims on inherited cores. This interpretation is consistent with both CSD and isotopic data sets.

WHAT CAN ISOTOPIC STUDIES OF MELT INCLUSIONS ADD TO OUR UNDERSTANDING OF MAGMA SYSTEMS?

Melt inclusions have long been held as key tools for unlocking magma sources (Lowenstern 2003) because they represent instantaneous samples of magma trapped in growing crystals (**Figure 9**). As such, just as with growth zones in crystals, they may present a stratigraphic (core-to-rim) record of magma composition evolution through time. In principle, magma elemental compositions can be recovered directly from analysis of homogeneous melt inclusions, in contrast to crystal growth zones, which have partitioned elements from the magma (and therefore require knowledge of partitioning behavior). In practice, crystallization of daughter crystals, or crystallization of the outer margin of the melt inclusion, can modify compositions significantly and needs to be accounted for (Danyushevsky et al. 2002).

By virtue of their small sizes (typically 10–100 μm), isotopic information has proved far more difficult to recover from melt inclusions than elemental information. Nevertheless, isotope compositions have the specific advantage that they are not compromised by crystallization, and there is no need for careful rehomogenization. With the advent of analytical techniques capable of recovering isotopic data from melt inclusions, a number of important studies have documented considerable isotopic diversity among melt inclusion populations.

Isotopic studies of melt inclusions in olivines and pyroxenes (individual inclusions or whole grain aggregates) have commonly shown ranges in isotope ratios, which far exceed those of the host bulk rocks (e.g. Saal et al. 1998, 2005; Yurimoto et al. 2004 for SW Pacific OIB; and Jochum et al. 2004, Kobayashi et al. 2004 for Hawaiian basalts; **Figure 10**). The diversity in melt inclusions is often accompanied by a trend to isotopic compositions, which are more contaminated than those of the host (although contamination trends in Pb isotope space are less straightforward than those involving Sr isotopes). This observation is not consistent with the notion that melt inclusions trapped in early-formed phases represent primitive aliquots of melt. It is consistent with the earliest stages of crystallization (where magmatic temperatures are high and the system may not have insulated itself with its own cumulate such that

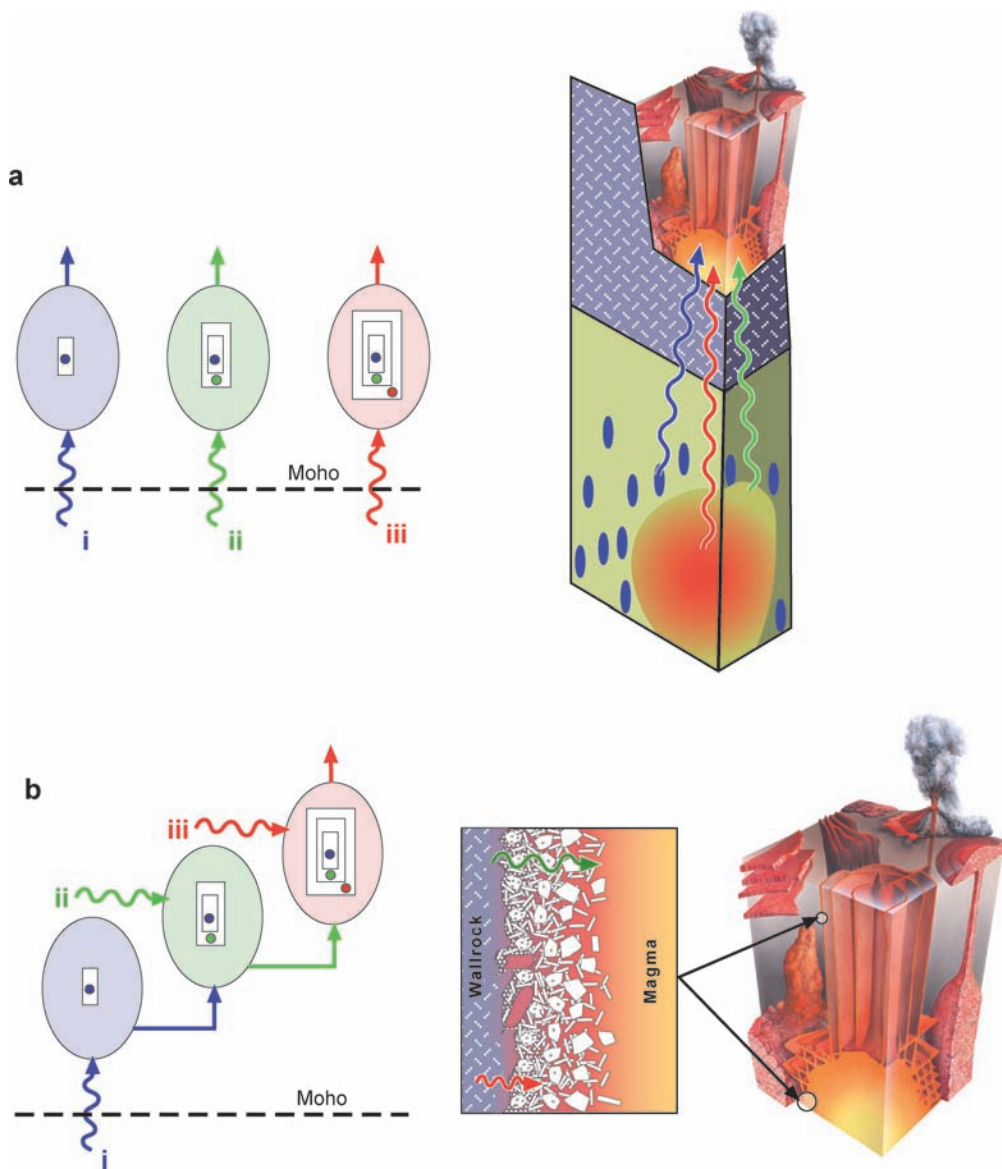


Figure 9

Schematic illustration of alternative interpretations of melt inclusion isotope data. (a) Melt inclusions are trapped from successive aliquots of magma (i, ii, and iii) derived from different mantle (sub Moho) sources. (b) The melt composition from which the crystal grows changes within the storage and delivery system owing to processes such as contamination and recharge from other parts of the system (cartoon adapted from Wolff et al. 1999). Note that in reality, relative to the system, either the crystal can stay in one place with the magma composition changing around it or the magma compositions can be fixed, with the crystal being transferred among different magma volumes in the system.

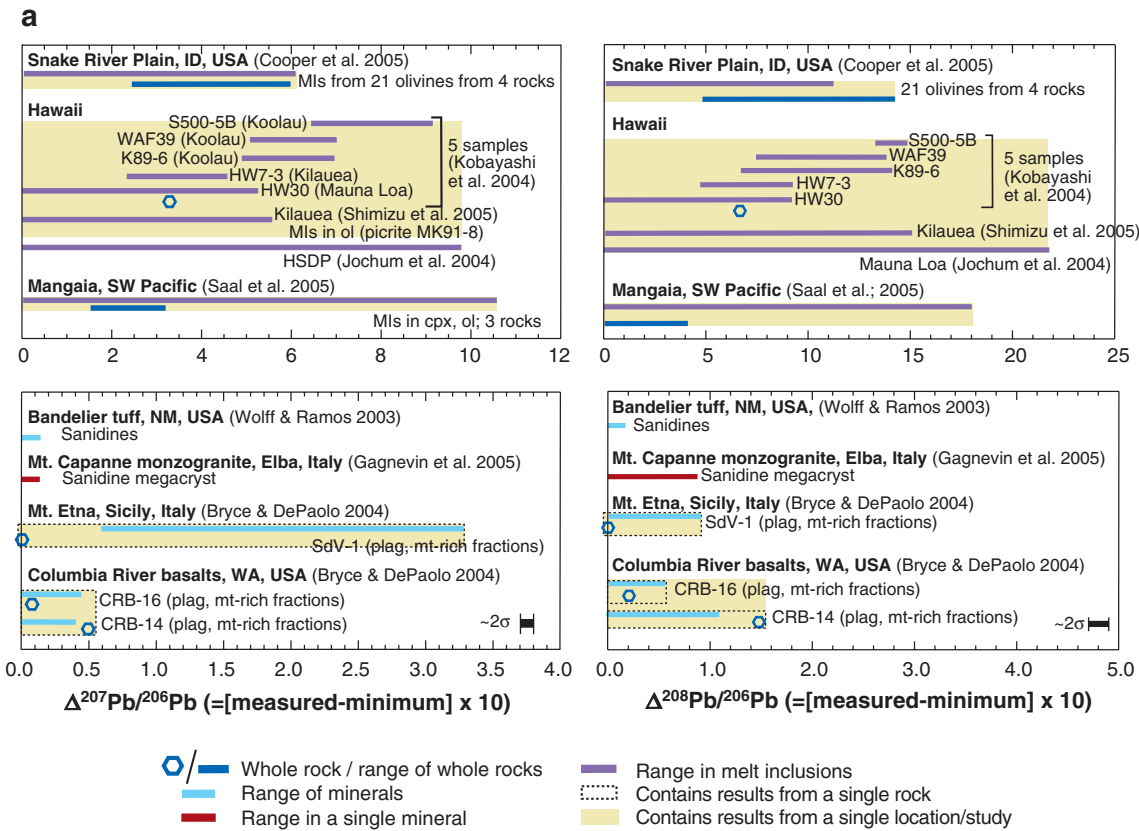


Figure 10

Compilation of data from minerals—either profiled for CIS, dissolved whole single crystals, or in some cases (e.g., Bryce & DePaolo 2004) aggregated and dissolved] and melt inclusions. Comparison is based on an x-axis scale that simply converts the isotopic ratios to ranges relative to the minimum value for each system, set as zero. (a) Pb isotopes and (b) Sr isotopes. Data sources as listed on figure. Abbreviations: WR = whole rock, MI = melt inclusion, cpx = - clinopyroxene, plag = plagioclase, mt = magnetite, apt = apatite, anh = anhydrite, ol = olivine

magma-wallrock contact is at its most extensive) involving significant contamination. Saal et al. (2005), for instance, suggest that the diversity of melt inclusions in olivines from Polynesia (**Figure 10a**) reflect interaction with and contamination by the oceanic lithosphere through which the magmas pass.

Olivine-hosted melt inclusions from a single NW Iceland ankaramite lava (**Figure 10b**) span 65% of the total $^{87}\text{Sr}/^{86}\text{Sr}$ range shown by OIB (contrasted with the whole-rock hosts, which cover only 5% of the global OIB range in $^{87}\text{Sr}/^{86}\text{Sr}$). Even larger Sr isotopic variations have been documented within olivine hosted MIs from the Baffin Iceland picrites (Harlou et al. 2006). The Sr isotopic range of these melt inclusions are three times that of the North Atlantic MORBs. Hence, these

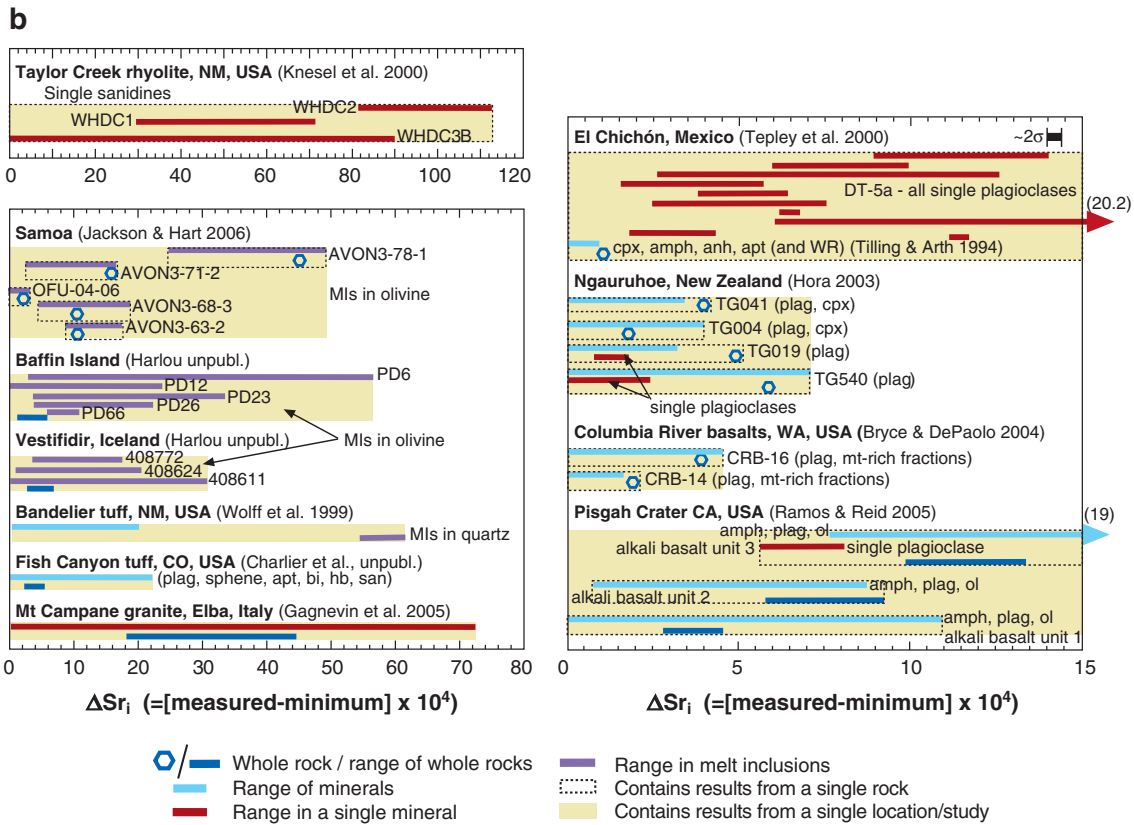


Figure 10

(Continued)

detailed Sr isotopic studies of individual melt inclusions evidently illustrate that they record chemical details that are not detectable in the host lavas.

Large isotopic variations among melt inclusion compositions are generated when a magma sequesters olivine phenocrysts that have crystallized in different parts of the system. Olivine entrapping melt inclusions in the central parts of a magma chamber or conduit (distal to the wall rock) may have an isotopic signature inherited from the source region, with little contamination. In contrast, melt inclusions trapped in crystals growing in boundary layers at the periphery of the magma storage and channeling system (where rising melts interact with the wall rock) may record large isotopic heterogeneities reflecting contributions from the wall rock lithologies encountered en route (Harlou et al. 2006).

Wolff et al. (1999) analyzed single inclusion-bearing quartz grains from the Bandelier Tuff (New Mexico, USA) for $^{87}\text{Sr}/^{86}\text{Sr}_i$. The melt inclusions have a higher $^{87}\text{Sr}/^{86}\text{Sr}$ than the host, which was interpreted to reflect crystal growth in an environment more contaminated than the main body of magma. Such an environment

might be adjacent to the chamber margin or dike/sill walls, where wallrock melts are mixed into an interaction zone. Such contact zones are the most likely place for crystallization to occur because they represent the location where the magma experiences the greatest relative undercooling, and they offer surfaces to promote nucleation and epitaxial growth and are preferential sites for melt inclusion entrapment (Wolff et al. 1999).

CIS VERSUS WHOLE-ROCK DATA AND THE ISSUE OF SCALE

A compilation of presently available mineral and melt inclusion CIS data is given in **Figure 10**. The figure compares whole rock data with the associated mineral and melt inclusion data. For ease of comparison, the x-axis is a relative scale, and a number of panels are used to illustrate adequately the dynamic range present; which is extraordinarily large relative to analytical precision. The compilation focuses on Pb (^{206}Pb , ^{207}Pb , and ^{208}Pb) and Sr isotopes (few CIS data are available for Nd, see Waight et al. (2000) for an example) and on common magmatic minerals (rather than accessories such as zircon). A wide spectrum of rock types are represented from basalts to rhyolites, and tectonic settings from intraplate to convergent margin. Rocks from both oceans and continents are represented.

Care must be taken in drawing conclusions from this comparison, which comprises a number of separate studies, using different techniques, and altogether amounting to a fairly limited volume of data. We must, for instance, bear in mind that most of the Pb isotope studies are on melt inclusions (by SIMS), only a few from single sanidine crystals, whereas the Sr isotope studies are dominated by single minerals (or mineral profiles by micromilling-TIMS) with fewer melt inclusion studies. Nevertheless we tentatively note the following:

1. There is no obvious link between composition and isotopic heterogeneity at the mineral scale. Basalts seem to show comparable diversity to rhyolites.
2. Similarly, there is no convincing sense that continental samples are more isotopically diverse at the mineral scale than oceanic samples.

What is convincing is that the intrarock isotopic diversity typically greatly exceeds that of the whole-rock suite from which the crystals and their melt inclusions have been derived. Thus, the isotopic diversity increases as the scale on which it is observed decreases. This observation was made for whole rocks by Zindler & Hart (1986) as a consequence of which they suggested that mantle heterogeneity existing at small lengthscales—as exemplified, for instance, in peridotite massifs such as Ronda—was averaged out during the melting process. The extension of their observation to isotopic diversity within single minerals can be explained by either of the following:

1. Isotopically diverse melts from the mantle are transferred to the lithosphere where they are mixed efficiently to average their compositions and result in a narrower range of isotopic compositions from the erupted rocks than from the input melts (cf **Figure 1**). In this case, crystals must grow before the melts are homogenized and the isotopic diversity of the inclusion suite is a better

- representative of the diversity of mantle sources than whole-rock compositions (e.g., Bryce & DePaolo 2004, Saal et al. 1998, Yurimoto et al. 2004; **Figure 10a**)
2. Isotopically (relatively) homogeneous melts from the mantle are transferred to the lithosphere where they interact with isotopically heterogeneous lithologies. In this case the mineral CIS profiles or inclusion suites do not reflect the diversity of primary melts, but rather are a secondary feature developed largely during differentiation (e.g., Ramos & Reid 2005; **Figure 10b**). Nevertheless, it may be possible to access the primary magma composition(s) through this approach by extrapolating toward the end-member compositions (**Figure 1**).

Distinguishing between the above alternatives is critical (although we should note that they need not be mutually exclusive). If it turns out that isotopic diversity is inherited from open-system processes during differentiation and ascent through the lithosphere, then we may be erroneously attributing compositional characteristics to mantle sources.

Mush: framework of crystals (cumulate) with interstitial melt

CUMULATE RECYCLING AND EVOLUTION OF MAGMAS TRANSITING THE CRUST

Danyushevsky et al. (2002) point out that melt inclusion populations in olivine commonly demand that crystals are aggregated following separate evolutionary histories. Indeed, it can be shown that crystal populations are invariably made up of chains and clusters of crystals to a certain degree, implying a recycling of crystal frameworks such as those developed in crystal mushes (Jerram et al. 2003). This conclusion is consistent with petrographic and geochemical observations such as those of Dungan & Davidson (2004) for Tatara-San Pedro Volcano (South Chile), Heath et al. (1998) for Soufriere Volcano (Lesser Antilles), and Price et al. (2005) for Ruapehu/Tongariro (New Zealand), showing that crystals are largely recycled from cannibalized cumulate, and with models of multiply staged crystallization and remobilization, such as the mush column model of Marsh (1998, 2004) and its precursors (Cox 1980, Thompson et al. 1972). Such mixing between “young” melts and older crystal cores can also satisfy chronological constraints raised by U-series disequilibria. Specifically, young ^{226}Ra - ^{232}Th ages reflect melts generated $\ll 8000$ years ago, which contributed to groundmass and crystal rims, whereas older ^{230}Th - ^{238}U ages on the same rocks are dominated by contributions from recycled older (>10 kyr) cumulate crystal cores (Turner et al. 2003).

Currently, popular models suggest that that much magma processing occurs deep in the crust driven by the thermal engine of magma emplaced near the Moho (Annen et al. 2006, Dufek & Bergantz 2006, Petford & Gallagher 2001, Price et al. 2005). Magma systems may inherit significant isotopic diversity from this stage of evolution as thermal considerations predict that it is where the magma is most capable of assimilating crust. However, predicted ascent paths for volatile-bearing magmas recross the liquidus, resulting in dissolution of the crystal cargo entrained from depth (Annen et al. 2006). There exists, then, an apparent paradox between the observation of core-to-rim isotope variation in crystals that requires the host magma to change its isotopic composition during crystal growth, and the expectation that significant

crystallization may take place largely in response to decompression during eruption (Blundy & Cashman 2005) rather than owing to cooling deeper in the system in an environment conducive to development of isotopic heterogeneity. These observations can, however, be reconciled in the following ways:

1. Isotopic diversity is transferred from the deep crust to shallow levels where it is stored in cumulates. On average, <20% of the magma flux from the mantle erupts at the surface (Crisp 1984); wholly crystallized material in the shallow-to-mid crust, is common.
2. Subsequent magmas intercept the precursor cumulates, remobilizing the crystals as antecrysts (**Figure 6**).
3. Partial dissolution of these crystals can change the isotopic composition of the host magma from which subsequent crystallization may occur.
4. On ascent to the surface, significant crystallization occurs both as microlites and epitaxially as rims to the antecrysts. This can represent volumetrically a major fraction of the total crystals (a 100 μm rim on a 2-mm-diameter crystal represents some 30% of its volume), and so can have significant leverage on melt elemental composition.

The key to establishing the evolution pathways of magmas confidently lies in integrating CIS approaches with textural quantification (as described above) and with careful P-T- $X_{\text{H}_2\text{O}}$ determinations of the crystal cargo and melt inclusion populations.

MICROSAMPLING AND FUTURE DIRECTIONS

The advent of multicollector mass spectrometry and gradual improvement of chemical techniques has given us the capacity to determine the isotopic composition of mineral materials at the subgrain scale, within the limitations summarized earlier. We argue that isotopic microsampling has opened up new avenues for understanding magmatic sources and processes, with a new level of detail and confidence that is obscured by traditional bulk rock approaches. The limitations on our capacity to analyze small samples are imposed largely by technical considerations, which may still see advances. In standard TIMS analysis, only a small fraction of the sample ($\ll 1\%$) is ionized and transmitted to the detector—>99% of the sample is effectively lost. Any increase in the ion flux at the detector over present capabilities would allow us to analyze smaller samples. Better signal-to-noise ratios would similarly lead to improved precision at smaller sample sizes and detectors that can operate in the cross-over area where signals are too intense for ion counting but not quite enough for good Faraday cup measurements. At the same time, direct in situ techniques such as LA-ICPMS could be improved by better filtering of interfering species (the purpose for which collision cells are being developed). Advances in the 3-D reconstruction of crystal populations through sectioning and imaging techniques (e.g., Mock & Jerram 2005, Gualda 2006) provide the exciting prospect of fully targeted microsampling where the true 3-D location of analysis is quantified, and specific aspects of the crystal population can be identified for analysis, further improving the spatial resolution of the data.

SUMMARY POINTS

1. Isotopic variations in magmatic minerals and their melt inclusions reflect isotopic variations in the magmas from which they crystallized. Thus, core-to-rim isotope profiles represent an evolutionary record of the magma from crystal nucleation to eruption/emplacement.
2. Crystals commonly do not spend their entire crystallization history in the magma in which they are finally hosted. They have typically grown in different places and at different times in the magma system (and can be referred to as antecrysts).
3. Recycling of earlier-formed cumulate phases appears to be an important process in aggregating antecrysts into magmas.
4. Integration of isotopic microsampling techniques with petrographic and geochemical approaches is important in fully constraining magma evolution—allowing us to correlate isotopic changes with events such as recharge and mixing (manifest in dissolution horizons and inclusion zones) and allowing us to evaluate the timescales of these processes (by diffusional modeling of element profiles across crystal growth zones).
5. The isotopic diversity observed through microsampling attests to the importance of open-system processes during magmatic differentiation.

ACKNOWLEDGMENTS

The research philosophies and methodologies reviewed here have been developed with the input of many colleagues, including George Bergantz, John Blundy, Mike Dungan, John Eichelberger, Laura Font, Catherine Ginibre, Chris Hawkesworth, Peter Holden, Kurt Knesel, Dougal Jerram, Bruce Marsh, Vikki Martin, Geoff Nowell, Graham Pearson, Frank Tepley, Simon Turner, Marge Wilson, John Wolff, and the whole ERUPT team. The manuscript benefited from comments by George Bergantz, John Gamble, Dougal Jerram, Simon Turner, and Tod Waight. Funding for the authors' work discussed in this review is provided by the National Science Foundation (USA), the Natural Environmental Research Council (UK), the European Union, the Danish Lithosphere Centre funded by the Danish National Research Foundation) and UCLA.

LITERATURE CITED

- Annen C, Blundy JD, Sparks RSJ. 2006. The genesis of intermediate and silicic magmas in deep crustal hot zones. *J. Petrol.* 47:505–39
- Bachmann O, Dungan MA, Lipman PW. 2002. The Fish Canyon magma body, San Juan Volcanic Field, Colorado: rejuvenation and eruption of an upper-crustal batholith. *J. Petrol.* 43:1469–503

- Bacon CR. 1986. Magmatic inclusions in silicic and intermediate volcanic rocks. *J. Geophys. Res.* 91:6091–112
- Barbey P, Ayalew D, Yirgu G. 2005. Insight into the origin of gabbro-dioritic cumulo-phyric aggregates from silicic ignimbrites: Sr and Ba zoning profiles of plagioclase phenocrysts from Oligocene Ethiopian Plateau rhyolite. *Contrib. Mineral. Petrol.* 149:233–45
- Bindeman IN. 2003. Crystal sizes in evolving silicic magma chambers. *Geology* 31:367–70
- Blundy J, Cashman K. 2005. Rapid decompression-driven crystallisation recorded by melt inclusions from Mount St. Helens volcano. *Geology* 33:793–96
- Brady JB. 1995. Diffusion data for silicate minerals, glasses, and liquids. I. *A Handbook of Physical Constants: Mineral Physics and Crystallography*, ed. TJ Ahrens, AGU Ref. Shelf Ser., Vol. 2:269–90. Washington, DC: Am. Geophys. Union
- Bryce JG, DePaolo DJ. 2004. Pb isotopic heterogeneity in basaltic phenocrysts. *Geochim. Cosmochim. Acta* 68:4453–68
- Cashman KV. 1990. Textural constraints on the kinetics of crystallization of igneous rocks. In *Reviews in Mineralogy and Geochemistry*, 24:259–314. Fredricksburg, VA: Geol. Soc. Am.
- Chadwick JP, Troll VR, Ginibre C, Morgan D, Gertisser R, et al. 2005. Xenocrystic material in arc volcanics: example from recent Merapi lavas. *Eos Trans. AGU* 86(52) Fall Meet. Suppl., Abstr. V13B-0530
- Charlier BLA, Wilson CJN, Lowenstern JB, Blake S, van Calsteren PW, Davidson JP. 2005. Magma generation at a large, hyperactive silicic volcano (Taupo, New Zealand) revealed by U–Th and U–Pb systematics in zircons. *J. Petrol.* 46:3–32
- Charlier BLA, Ginibre C, Morgan D, Nowell GM, Pearson DG, et al. 2006. Methods for the microsampling and analysis of strontium and rubidium isotopes at single crystal scale for petrological and geochronological applications. *Chem. Geol.* 232:114–33
- Cherniak DJ, Watson EB. 1994. A study of strontium diffusion in plagioclase using Rutherford backscattering spectroscopy. *Geochim. Cosmochim. Acta* 58:5179–90
- Christensen JN, DePaolo DJ. 1993. Timescale of large volume silicic magma systems: Sr isotopic systematics of phenocrysts and glass from the Bishop Tuff, Long Valley California. *Contrib. Mineral. Petrol.* 113:100–14
- Christensen JN, Halliday AN. 1996. Rb–Sr ages and Nd isotopic compositions of melt inclusions from the Bishop Tuff and the generation of silicic magma. *Earth Planet. Sci. Lett.* 144:547–61
- Christensen JN, Halliday AN, Lee D, Hall CM. 1995. In situ Sr isotopic analysis by laser ablation. *Earth Planet. Sci. Lett.* 136:79–85
- Christensen JN, Rosenfeld JL, DePaolo DJ. 1989. Rates of tectonometamorphic processes from rubidium and strontium isotopes in garnet. *Science* 224:1465–69
- Cioni R, Civetta L, Marianelli P, Metrich N, Santacroce R, Sbrana A. 1995. Compositional layering and syn-eruptive mixing of a periodically refilled shallow magma chamber—the AD-79 Plinian eruption of Vesuvius. *J. Petrol.* 36:739–76
- Clynne MA. 1999. A complex magma mixing origin for rocks erupted in 1915, Lassen Peak, California. *J. Petrol.* 40:105–32

- Connelly JN, Thrane K. 2005. Rapid determination of Pb isotopes to define Precambrian allochthonous domains: an example from West Greenland. *Geology* 33:953–56
- Cooper LB, Reid MR, Bryce JG. 2005. Pb isotope heterogeneity between olivine-hosted melt inclusions, Eastern Snake river plain, Idaho. *Geochim. Cosmochim. Acta* 69/10S:A98 (Abstr.)
- Costa F, Chakraborty S, Dohmen R. 2003. Diffusion coupling between trace and major elements and a model for calculation of magma residence times using plagioclase. *Geochim. Cosmochim. Acta* 67:2189–200
- Costa F, Dungan MA. 2005. Short time scales of magmatic assimilation from diffusion modeling of multiple elements in olivine. *Geology* 33:837–40
- Cox KG. 1980. A model for flood basalt volcanism. *J. Petrol.* 21:621–50
- Crisp JA. 1984. Rates of magma emplacement and volcanic output. *J. Volcanol. Geotherm. Res.* 20:177–211
- Danyushevsky LV, Sokolov S, Falloon TJ. 2002. Melt inclusions in olivine phenocrysts: using diffusive re-equilibration to determine the cooling history of a crystal, with implications for the origin of olivine-phyric volcanic rocks. *J. Petrol.* 43:1651–71
- Davidson JP, Font L, Charlier BLA, Tepley FJ III. 2007. Mineral-scale. Sr isotope variation in plutonic rocks—a tool for unraveling the evolution of magma systems. *Proc. R. Soc. Edinb.* In press
- Davidson JP, Tepley FJ III. 1997. Recharge in volcanic systems; evidence from isotope profiles of phenocrysts. *Science* 275:826–29
- Davidson JP, Tepley FJ III, Knesel KM. 1998. Crystal isotope stratigraphy; a method for constraining magma differentiation pathways. *Eos Trans. Am. Geophys. Union* 79:185, 189, 193
- Davidson JP, Tepley FJ III, Palacz Z, Main S. 2001. Magma recharge, contamination and residence times revealed by *in situ* laser ablation isotopic analysis of feldspar in volcanic rocks. *Earth Planet. Sci. Lett.* 182:427–42
- Dickin AP. 2005. *Radiogenic Isotope Geology*. Cambridge, UK: Cambridge Univ. Press. 2nd ed.
- Dufek J, Bergantz GW. 2006. Lower crustal magma genesis and preservation: a stochastic framework for the evaluation of basalt–crust interaction. *J. Petrol.* 46:2167–95
- Duffield WA, Ruiz J. 1992. Compositional gradients in large volume reservoirs of silicic magma as evidenced by ignimbrites versus Taylor Creek Rhyolite lava domes. *Contrib. Mineral. Petrol.* 110:192–210
- Duffield WA, Ruiz J. 1994. A model to help explain Sr-isotope disequilibrium between feldspar phenocrysts and melt in large-volume silicic magma systems. *U.S. Geol. Surv. Open-File Rep.* 94-423
- Dungan MA, Davidson JP. 2004. Partial assimilative recycling of the mafic plutonic roots of arc volcanoes: an example from the Chilean Andes. *Geology* 32:773–76
- Eichelberger JC. 1978. Andesitic volcanism and crustal evolution. *Nature* 275:21–27
- Espíndola JM, Macías JL, Tilling RI, Sheridan MF. 2000. Volcanic history of El Chichón Volcano (Chiapas, Mexico) during the Holocene, and its impact on human activity. *Bull. Volcanol.* 62:90–104

- Faure G. 1986. *Principles of Isotope Geology*. New York: Wiley
- Gagnevin D, Daly JS, Poli G, Morgan D. 2005a. Microchemical and Sr isotopic investigation of zoned K-feldspar megacrysts: insights into the petrogenesis of a plutonic system and disequilibrium processes during crystal growth. *J. Petrol.* 46:1689–724
- Gagnevin D, Daly JS, Waight TE, Morgan D, Poli G. 2005b. Pb isotopic zoning of K-feldspar megacrysts determined by laser ablation multiple-collector ICP-MS: insights into granite petrogenesis. *Geochim. Cosmochim. Acta* 69:1899–915
- Geist DJ, Myers JD, Frost CD. 1988. Megacryst-bulk rock isotopic disequilibrium as an indicator of contamination process: the Edgcombe Volcanic Field, SE Alaska. *Contrib. Mineral. Petrol.* 99:105–12
- Giletti BJ, Casserly ED. 1994. Strontium diffusion kinetics in plagioclase feldspars. *Geochim. Cosmochim. Acta* 58:3785–93
- Ginibre C, Kronz A, Wörner G. 2002. High-resolution quantitative imaging of plagioclase composition using accumulated Back-Scattered Electron images: new constraints on oscillatory zoning. *Contrib. Mineral. Petrol.* 142:436–48
- Ginibre C, Wörner G, Kronz A. 2004. Structure and dynamics of the Laacher See magma chamber (Eifel, Germany) from major and trace element zoning in sanidine: a cathodoluminescence and electron microprobe study. *J. Petrol.* 45:2197–23
- Grove TL, Gerlach D, Sando TW. 1982. Origin of calc-alkaline series lavas at Medicine Lake Volcano by fractionation, assimilation and mixing. *Contrib. Mineral. Petrol.* 80:160–82
- Gualda GAR. 2006. Crystal size distributions derived from 3D datasets: sample size versus uncertainties. *J. Petrol.* 47:1245–54
- Halliday AN, Fallick AE, Hutchinson J, Hildreth W. 1984. A Nd, Sr and O isotopic investigation into the causes of chemical and isotopic zonation in the Bishop Tuff, California. *Earth Planet. Sci. Lett.* 68:379–91
- Halliday AN, Mahood GA, Holden P, Metz JM, Dempster TJ, Davidson JP. 1989. Evidence for long residence times of rhyolitic magma in the Long Valley magmatic system: the isotopic record in precaldera lavas of Glass Mountain. *Earth Planet. Sci. Lett.* 94:274–90
- Hanchar JM, Hoskin PWO. 2003. Modern methods of igneous petrology: understanding magmatic processes. In *Zircon. Reviews in Mineralogy and Geochemistry*, Vol. 53, ed. J Nicholls and JK Russell. Fredricksburg, VA: Mineral. Soc. Am. 500 pp.
- Harlou R, Pearson DG, Davidson JP, Kamenetsky VS, Yaxley GM. 2006. Source variability and crustal contamination of the Baffin Island picrites—coupled Sr isotope and trace element study of individual melt inclusions. *Geochim. Cosmochim. Acta* 70/18S:A231 (Abstr.)
- Harlou R, Pearson DG, Nowell GM, Davidson JP, Kent AJR. 2005. Sr isotope studies of melt inclusions by TIMS. *Geochim. Cosmochim. Acta* 69/10S:A380 (Abstr.)
- Heath E, Turner SP, Macdonald R, Hawkesworth CJ, Van Calsteren P. 1998. Long magma residence times at an island arc volcano (Soufrière, St. Vincent) in the Lesser Antilles: evidence from ^{238}U - ^{230}Th isochron dating. *Earth Planet. Sci. Lett.* 160:49–63

- Hervig RL, Dunbar NW. 1992. Cause of chemical zoning in the Bishop (California) and Bandelier (New Mexico) magma chambers. *Earth Planet. Sci. Lett.* 111:97–108
- Higgins MD. 2000. Measurement of crystal size distributions. *Am. Mineral.* 85:1105–16
- Hobden BJ. 1997. *Modelling magmatic trends in time and space: eruptive and magmatic history of Tongariro volcanic complex, New Zealand*. PhD thesis. Univ. Canterbury. 508 pp.
- Hobden BJ, Houghton BF, Davidson JP, Weaver SD. 1999. Small and short-lived magma batches at composite volcanoes: time windows at Tongariro volcano, New Zealand. *J. Geol. Soc. London* 156:865–68
- Hobden BJ, Houghton BF, Nairn IA. 2002. Growth of a young, frequently active composite cone: Ngauruhoe volcano, New Zealand. *Bull. Volcanol.* 64:392–409
- Hora JM. 2003. *Magmatic differentiation processes at Ngauruhoe Volcano, New Zealand: constraints from chemical, isotopic and textural analysis of plagioclase crystal zoning*. MSc thesis. Univ. Calif., Los Angeles
- Ireland TR. 1995. Ion microprobe mass spectrometry: techniques and applications in cosmochemistry, geochemistry, and geochronology. In *Advances in Analytical Geochemistry*, ed. M Hyman, M Rowe, 2:1–118. Middlesex: England: JAI
- Jackson MG, Hart SR. 2006. Strontium isotopes in melt inclusions from Samoan basalts: implications for heterogeneity in the Samoan plume. *Earth Planet. Sci. Lett.* 245:260–77
- Jerram DA, Cheadle MC, Philpotts AR. 2003. Quantifying the building blocks of igneous rocks: are clustered crystal frameworks the foundation? *J. Petrol.* 44:2033–51
- Jochum KP, Stoll B, Herwig K, Hofmann AW. 2004. Pb isotopes and trace elements in melt inclusions from Hawaiian basalts using LA-ICPMS and SR-XRF. *Geochim. Cosmochim. Acta* 68/11S:A564 (Abstr.)
- Kennedy BP, Klaue A, Blum JD, Folt CL, Nislow KH. 2002. Reconstructing the lives of fish using Sr isotopes in otoliths. *Can. J. Fish. Aquat. Sci.* 59:925–29
- Knesel KM, Davidson JP, Duffield WA. 1999. Evolution of silicic magma through assimilation and subsequent recharge: evidence from Sr isotopes in sanidine phenocrysts, Taylor Creek rhyolite, NM. *J. Petrol.* 40:773–86
- Kobayashi K, Tanaka R, Moriguti K, Shimizu N, Nakamura E. 2004. Lithium, boron, and lead isotope systematics of glass inclusions in olivines from Hawaiian lavas: evidence for recycled components in the Hawaiian plume. *Chem. Geol.* 212:143–61
- Koyaguchi T. 1986. Evidence for two-stage mixing in magmatic inclusions and rhyolitic lava domes on Nijima Island, Japan. *J. Volcanol. Geotherm. Res.* 29:71–98
- Lowenstern JB. 2003. Melt inclusions come of age: volatiles, volcanoes, and Sorby's legacy, I. In *Melt Inclusions in Volcanic Systems: Methods, Applications and Problems*, ed. B De Vivo, RJ Bodnar, *Developments in Volcanology* 5:1–22. Amsterdam: Elsevier
- Marsh BD. 1988. Crystal size distribution (CSD) in rocks and the kinetics and dynamics of crystallization I. Theory. *Contrib. Mineral. Petrol.* 99:277–91

- Marsh BD. 1998. On the interpretation of crystal size distributions in magmatic systems. *J. Petrol.* 39:553–99
- Marsh BD. 2004. A magmatic mush column Rosetta Stone: the McMurdo Dry Valleys of Antarctica. *Eos Trans.* 85:497, 502
- Mathez EA, Waight TE. 2003. Lead isotopic disequilibrium between sulfide and plagioclase in the Bushveld Complex and the chemical evolution of large layered intrusions. *Geochim. Cosmochim. Acta* 67:1875–88
- McGee JJ, Tilling RI. 1983. 1982 and pre1982 magmatic products of El Chichón volcano, Chiapas, Mexico. *Eos Trans. Am. Geophys. Union* 64:893
- McGee JJ, Tilling RI, Duffield WA. 1987. Petrologic characteristics of the 1982 and pre1982 eruptive products of El Chichón volcano, Chiapas, Mexico. *Geof. Int.* 26-1:85–108
- Mock A, Jerram DA. 2005. Crystal size distributions (CSD) in three dimensions: insights from the 3D reconstruction of a highly porphyritic rhyolite? *J. Petrol.* 46:1525–41
- Morgan D, Blake S. 2006. Magmatic residence times of zoned phenocrysts: introduction and application of the binary element diffusion modelling (BEDM) technique. *Contrib. Mineral. Petrol.* 151:58–70
- Morgan D, Blake S, Rogers N, DeVivo B, Rolandi G, et al. 2004. Timescales of crystal residence and magma chamber volume from modeling of diffusion profiles in phenocrysts: Vesuvius 1944. *Earth Planet. Sci. Lett.* 222:933–46
- Morgan D, Chertkoff DG, Jerram DA, Davidson JP, Francalanci L. 2005. What's in a whole rock analysis? Integrating crystal size distributions and micro-scale isotopic variations at Stromboli Volcano. *Eos Trans. Am. Geophys. Union Fall Meet. Suppl.*, 86(52):V12A-08 (Abstr.)
- Morgan DJ, Blake S, Rogers NW, De Vivo B, Rolandi G, Davidson JP. 2006. Magma recharge at Vesuvius in the century prior to the eruption of AD 79. *Geology* 34:845–48
- Müller W. 2003. Strengthening the link between geochronology, textures and petrology. *Earth Planet. Sci. Lett.* 206:237–51
- Müller W, Aerden D, Halliday AN. 2000. Isotopic dating of strain fringe increments: duration and rates of deformation in shear zones. *Science* 288:2195–98
- Müller W, Kelley SP, Villa IM. 2002. Dating fault-generated pseudotachylytes: comparison of $^{40}\text{Ar}/^{39}\text{Ar}$ stepwise heating, laser-ablation and Rb-Sr-microsampling analyses. *Contrib. Mineral. Petrol.* 144:57–77
- Neal CR, Davidson JP, McKeegan KD. 1995. Geochemical analysis of small samples. *U.S. Nation. Rep. IUGG (1991–1994) Rev. Geophys., Suppl.*, pp. 25–32
- Pagel M, Barbin V, Blanc P, Ohnenstetter D, eds. 2000. *Cathodoluminescence in Geosciences*. Berlin: Springer Verlag. 227 pp.
- Perini G, Tepley FJ III, Davidson JP, Conticelli S. 2003. The origin of K-feldspar megacrysts hosted in alkaline potassic rocks from central Italy: a track for low-pressure processes in mafic magmas. *Lithos.* 66:223–40
- Petford N, Gallagher K. 2001. Partial melting of mafic (amphibolitic) lower crust by periodic influx of basaltic magma. *Earth Planet. Sci. Lett.* 193:483–89

- Price RC, Gamble JA, Smith IEM, Stewart RB, Eggins S, Wright IC. 2005. An integrated model for the temporal evolution of andesites and rhyolites and crustal development in New Zealand's North Island. *J. Volcanol. Geotherm. Res.* 140:1–24
- Ramos FC, Reid MR. 2005. Distinguishing melting of heterogeneous mantle sources from crustal contamination: insights from Sr isotopes at the Phenocryst Scale, Pisgah Crater, California. *J. Petrol.* 46:999–1012
- Ramos FC, Wolff JA, Tollstrup DL. 2004. Measuring $^{87}\text{Sr}/^{86}\text{Sr}$ variations in minerals and groundmass from basalts using LA-MC-ICPMS. *Chem. Geol.* 211:135–58
- Ramos FC, Wolff JA, Tollstrup DL. 2005. Sr isotope disequilibrium in Columbia River flood basalts: evidence for rapid shallow-level open system processes. *Geology* 33:457–60
- Saal AE, Hart SR, Shimizu N, Hauri EH, Layne GD. 1998. Pb isotopic variability in melt inclusions from oceanic island basalts, Polynesia. *Science* 282:1481–84
- Saal AE, Hart SR, Shimizu N, Hauri EH, Layne GD, Eiler JM. 2005. Pb isotopic variability in melt inclusions from the EMI-EMII-HIMU mantle end-members and the role of oceanic lithosphere. *Earth Planet. Sci. Lett.* 240:605–20
- Shimizu N, Kobayashi K, Sisson T, Layne G, Nakamura E, Kurz M. 2005. Evolution of diverse mantle sources for the Kilauea Volcano over 270 Ka. *Eos Trans. Am. Geophys. Union Fall Meet. Suppl.*, 86(52):V22A-07 (Abstr.)
- Simonetti A, Bell K. 1993. Isotopic disequilibrium in clinopyroxenes from nephelinitic lavas, Napak Volcano, eastern Uganda. *Geology* 21:243–46
- Sisson T, Grove TL. 1993. Experimental investigations of the role of H_2O in calc-alkaline differentiation and subduction zone magmatism? *Contrib. Mineral. Petrol.* 113:143–66
- Tepley FJ III, Davidson JP. 2003. Mineral-scale Sr-isotope constraints on magma evolution and chamber dynamics in the Rum Layered Intrusion, Scotland. *Contrib. Mineral. Petrol.* 145:628–41
- Tepley FJ III, Davidson JP, Clyne MA. 1999. Magmatic interactions as recorded in plagioclase phenocrysts of Chaos Crags, Lassen Volcanic Center, California. *J. Petrol.* 40:787–806
- Tepley FJ III, Davidson JP, Tilling RI, Arth JG. 2000. Magma mixing, recharge and eruption histories recorded in plagioclase phenocrysts from El Chichón Volcano, Mexico. *J. Petrol.* 41:1397–411
- Thirlwall MF. 1997. Thermal ionisation mass spectrometry (TIMS). In *Modern Analytical Geochemistry: An Introduction to Quantitative Chemical Analysis Techniques for Earth, Environment and Materials Scientists*, ed. RCO Gill, pp. 135–53. Harlow, Essex, UK: Longman
- Thompson RN, Esson J, Dunham AC. 1972. Major element chemical variation in the Eocene lavas of the Isle of Skye, Scotland. *J. Petrol.* 13:219–53
- Tilling RI, Arth JG. 1994. Sr and Nd isotopic compositions of sulfur-rich magmas of El Chichón Volcano, Mexico. *IAVCEI Congr., Middle East Tech. Univ. Dep. Geol. Eng., Spec. Publ. 2* (Abstr.)
- Tilling RI, Rubin M, Sigurdsson H, Carey S, Duffield WA, Rose WI. 1984. Holocene eruptive activity of El Chichón Volcano, Chiapas, Mexico. *Science* 224:747–49

- Tsuchiyama A. 1985. Dissolution kinetics of plagioclase in the melt of the system diopside-albite-anorthite, and the origin of dusty plagioclase in andesites. *Contrib. Mineral. Petrol.* 89:1–16
- Turner S, George R, Jerram DA, Carpenter N, Hawkesworth CJ. 2003. Case studies of plagioclase growth and residence times in island arc lavas from Tonga and the Lesser Antilles, and a model to reconcile discordant age information. *Earth Planet. Sci. Lett.* 214:279–94
- Tyrell S, Haughton PDW, Daly JS, Kokfelt TF, Gagnevin D. 2006. The use of common Pb isotopic composition of detrital K-feldspar grains as a provenance tool and its application to Upper Carboniferous palaeodrainages in Northern England. *J. Sed. Res.* 76:324–45
- Waight TE, Baker J, Peate D. 2002. Sr isotope ratio measurements by double-focusing MC-ICPMS: techniques, observations and pitfalls. *Int. J. Mass Spectr.* 221:229–44
- Waight TE, Maas R, Nicholls IA. 2000. Fingerprinting feldspar phenocrysts using crystal isotopic composition stratigraphy: implications for crystal transfer and magma mingling in S-type granites. *Contrib. Mineral. Petrol.* 139:227–39
- Waight TE, Wiebe RA, Krogstad EJ, Walker RJ. 2001. Isotopic responses to basaltic injections into silicic magma chambers: a whole rock and microsampling study of macrorhythmic units in the Pleasant Bay layered gabbro-diorite complex, Maine, USA. *Contrib. Mineral. Petrol.* 142:323–35
- Walker D, Shibata T, Delong SE. 1979. Abyssal tholeiites from the Oceanographer Fracture-Zone. 2. Phase-equilibria and mixing. *Contrib. Mineral. Petrol.* 70:111–25
- Wallace GS, Bergantz GW. 2005. Reconciling heterogeneity in crystal zoning data: an application of shared characteristic diagrams at Chaos Crags, Lassen Volcanic Center, California. *Contrib. Mineral. Petrol.* 149:98–112
- Wolff JA, Ramos F. 2003. Pb isotope variations among Bandelier Tuff feldspars: no evidence for a long-lived silicic magma chamber. *Geology* 31:533–36
- Wolff JA, Ramos FC, Davidson JP. 1999. Sr isotope disequilibrium during differentiation of the Bandelier Tuff, New Mexico: constraints on the crystallization of a large rhyolitic magma chamber. *Geology* 27:495–98
- Yurimoto H, Kogisu T, Abe K, Barszczus HG, Utsonimiy A, Maruyama S. 2004. Lead isotopic compositions in olivine-hosted melt inclusions from HIMU basalts and possible link to sulfide components. *Phys. Earth Planet. Int.* 146:231–42
- Zellmer GF, Blake S, Vance D, Hawkesworth C, Turner S. 1999. Plagioclase residence times at two island arc volcanoes (Kameni Islands, Santorini, and Soufriere, St Vincent) determined by Sr diffusion systematics. *Contrib. Mineral. Petrol.* 136:345–57
- Zellmer GF, Clavero JE. 2006. Using trace element correlation patterns to decipher a sanidine crystal growth chronology: an example from Taapaca volcano, Central Andes. *J. Volcanol. Geotherm. Res.* 156:291–301
- Zindler A, Hart S. 1986. Chemical Geodynamics. *Annu. Rev. Earth Planet. Sci.* 14:493–571

RELATED RESOURCES

Bill White's online geochemistry text: <http://www.geo.cornell.edu/geology/classes/geo455/Chapters.HTML>

TiMAG (textural and isotopic microanalysis group) at the University of Durham: <http://www.dur.ac.uk/earth.sciences/research/research.groups/timag/>